

# Numerical analysis of thermal-slip and diffusion-slip flows of a binary mixture of hard-sphere molecular gases

Shigeru Takata,<sup>a)</sup> Shugo Yasuda, Shingo Kosuge, and Kazuo Aoki  
*Department of Aeronautics and Astronautics, Graduate School of Engineering, Kyoto University,  
Kyoto 606-8501, Japan*

(Received 7 April 2003; accepted 15 September 2003; published 3 November 2003)

The thermal-slip (thermal-creep) and the diffusion-slip problems for a binary mixture of gases are investigated on the basis of the linearized Boltzmann equation for hard-sphere molecules with the diffuse reflection boundary condition. The problems are analyzed numerically by the finite-difference method incorporated with the numerical kernel method, which was first proposed by Sone, Ohwada, and Aoki [Phys. Fluids A **1**, 363 (1989)] for a single-component gas. As a result, the behavior of the mixture is clarified accurately not only at the level of the macroscopic variables but also at the level of the velocity distribution function. In addition, accurate formulas of the thermal-slip and the diffusion-slip coefficients for arbitrary values of the concentration of a component gas are constructed by the use of the Chebyshev polynomial approximation. © 2003 American Institute of Physics. [DOI: 10.1063/1.1624075]

## I. INTRODUCTION

When a gas is slightly rarefied or the Knudsen number is small, the overall behavior of the gas around solid bodies can be described by a system of fluid-dynamic-type equations with terms of gas rarefaction effect and slip (or jump) condition for the flow velocity (or the temperature). Here, the Knudsen number  $Kn$  is the ratio of the mean free path of the gas molecules to the reference length. The solution of the system is required to be corrected in a thin layer adjacent to the solid-body surface. The layer is of the thickness of a few mean free paths of the gas molecules and is called the Knudsen layer. The physical variables are subject to appreciable change there in the direction normal to the surface. These features were clarified by a systematic asymptotic analysis of the Boltzmann equation for small Knudsen numbers (Sone's asymptotic theory; see, for instance, Refs. 1–4). The slip of flow (or the jump of temperature) and the Knudsen layer are considered as typical effects of gas rarefaction because they vanish when the continuum limit  $Kn \rightarrow 0$  is taken. This is a common understanding irrespective of whether the gas is pure or not.

In the meantime, Takata and Aoki<sup>5</sup> recently studied the steady behavior of a binary mixture of a vapor and a non-condensable gas around condensed phases of the vapor on the basis of kinetic theory. They carried out an asymptotic analysis of the Boltzmann equation for small Knudsen numbers and derived the fluid-dynamic-type system which describes the behavior of the mixture in the situation where the Mach number of the flow is as small as the Knudsen number while the temperature variation of the condensed phase may be large. Contrary to the common understanding, the derived system shows that the slip condition for the flow velocity is necessary even in describing the behavior of the mixture in

the continuum limit. This is an example of the recently discovered effect of gas rarefaction which remains at vanishing Knudsen number;<sup>6</sup> this phenomenon was termed the ghost effect (see Refs. 4, 7, and 8 for details). The present paper is intended to provide accurate data of the slip boundary condition which causes the ghost effect in the mixture in a wide class of physical situations studied in Ref. 5.

According to Ref. 5, the slip condition in the fluid-dynamic-type system derived there can be obtained by the analysis of the thermal-slip (thermal-creep)<sup>9</sup> and the diffusion-slip<sup>10</sup> flows of a mixture over a plane wall. The former is the flow of the mixture induced along the wall by a uniform gradient of the wall temperature along its surface, and the latter is that induced along the wall by a uniform gradient of the concentration of a component gas along the surface. These are both fundamental problems in rarefied gas dynamics. In the present study, we try to carry out an accurate numerical analysis of these problems on the basis of the linearized Boltzmann equation for hard-sphere molecules. An accurate finite-difference method for the linearized Boltzmann equation for a single-component hard-sphere gas was developed more than a decade ago<sup>11,12</sup> and has been applied to various fundamental problems (e.g., Refs. 13–24). The method was recently extended to a binary gas mixture in Ref. 25. We basically use this method in the present study.

The aim of the present study is twofold: first, to complete the slip boundary conditions for the fluid-dynamic-type equations mentioned above, and second, to establish numerical solutions of the linearized Boltzmann equation that serve as the standard solution to the two fundamental problems. For the first aim, we need the slip conditions for arbitrary values of the local concentration of a component gas because it generally varies along the boundary. This means that we need to obtain the solutions of the two slip-flow problems for arbitrary values of the background concentration. Therefore, we construct the solutions in such a way that the results for

<sup>a)</sup>Electronic mail: takata@aero.mbox.media.kyoto-u.ac.jp

any value of the background concentration can be obtained immediately. As mentioned above, the numerical method used in the present study is essentially the same as that developed in the Ref. 25, where the diffusion-slip problem has been investigated. In this reference, however, the solution was obtained for several values of the background concentration, not for its arbitrary values. Moreover, the information given there is limited because the paper is a contribution to the conference proceedings with limited space. In the present paper, we reanalyze the problem, parallel to the analysis of the thermal-slip problem, in a way appropriate to our purpose and present the results for both problems (we will omit some results concerning the diffusion-slip flow that overlap with Ref. 25). We will also describe the method of solution in a self-contained manner, since it is not given in Ref. 25.

Here, we make a brief remark on the second aim mentioned above. The two slip flows considered here have long been known<sup>9,10</sup> and have been investigated in many papers including some pioneering works<sup>26,27</sup> at the early stage of the modern kinetic theory (e.g., Refs. 12, 25, 28–40). Concerning gas mixtures, however, the existing works (except Ref. 25), such as the works based on moment and variational methods and on model equations, are of an approximate nature, and the direct numerical analysis has been avoided because of the complexity of the Boltzmann equation. In such circumstances, we try to solve the linearized Boltzmann equation straightforwardly to obtain reliable numerical solutions, restricting ourselves to the hard-sphere molecular model, which is not necessarily realistic but is the most fundamental model in kinetic theory. Such solutions will serve to assess other approximate methods. In particular, approximate methods aiming at obtaining slip coefficients for more realistic molecular models,<sup>34,38,39</sup> which will be useful in practical applications, can be validated to some extent by comparing their results for hard-sphere molecules with the present result.

The paper is organized as follows. First the problems are formulated in Sec. II. Then preliminary analysis is performed in Sec. III, where the similarity solution and the expression of the collision integrals in terms of the integral kernel are introduced. The numerical method is developed on the basis of this expression in Sec. IV. The results are given and the discussions are made in Sec. V. The data of computation are summarized in Sec. VI.

## II. FORMULATION OF THE PROBLEM

### A. Problem

We consider a semi-infinite expanse of a binary mixture of gases, gas A and gas B, over a plane wall. The wall is located at  $X_1=0$ , and the mixture occupies the region  $X_1 > 0$ , where  $X_i$  is the rectangular coordinate system. We will investigate the steady behavior of the mixture in the following situations.

**Problem I:** The wall is kept at temperature  $T_0 + \tilde{C}_I X_2$  with  $\tilde{C}_I$  being a constant. Far from the wall, the state of the mixture is independent of  $X_1$ , the pressure of the mixture and the concentration of gas A (the number fraction of the

molecules of gas A) are uniform, and the temperature of the mixture is the same as that of the wall  $T_0 + \tilde{C}_I X_2$ , i.e., it has a uniform gradient in the  $X_2$ -direction.

**Problem II:** The wall is kept at a uniform temperature  $T_0$ . Far from the wall, the state of the mixture is independent of  $X_1$ , the pressure of the mixture is uniform, its temperature is also uniform and is the same as that of the wall  $T_0$ , and the concentration  $X^A$  of gas A has a uniform gradient in the  $X_2$ -direction (thus the concentration  $X^B$  of gas B has a uniform gradient of the same magnitude in the opposite direction, because  $X^B = 1 - X^A$  by definition).

Problem I is called the thermal-slip problem, and problem II the diffusion-slip problem.

In what follows, the pressure of the mixture at infinity ( $X_1 \rightarrow \infty$ ) is denoted by  $p_0$ . The concentration of gas A (or gas B) at infinity is denoted by  $X_0^A$  (or  $X_0^B$ ) in problem I, and by  $X_0^A + \tilde{C}_{II}^A X_2$  (or  $X_0^B + \tilde{C}_{II}^B X_2$ ) in problem II. Note that the relations  $X_0^B = 1 - X_0^A$  and  $\tilde{C}_{II}^B = -\tilde{C}_{II}^A$  hold by definition. The superscripts  $\alpha$ ,  $\beta$ , and  $\gamma$  are symbolically used to represent the gas species, i.e.,  $\alpha, \beta, \gamma = A, B$ .

In the analysis, we make the following assumptions: (i) the molecules of gas  $\alpha$  are hard spheres of mass  $m^\alpha$  and diameter  $d^\alpha$  and they collide elastically each other; (ii) the behavior of the mixture is described by the Boltzmann equation and the diffuse reflection condition for the reflected molecules on the wall; and (iii) the magnitude of the gradient of temperature in problem I and that of concentration in problem II are so small that the equations and boundary conditions can be linearized around the reference equilibrium state at rest with temperature  $T_0$  and pressure  $p_0$  of the mixture and concentration  $X_0^\alpha$  of gas  $\alpha$ .

### B. Basic equation and boundary condition

We first summarize the main notation used in the paper. The  $n_0$  is the reference molecular number density of the mixture and is defined by  $n_0 = p_0 / kT_0$ , where  $k$  is Boltzmann's constant. The  $l_0$  is the mean free path of the molecules in the equilibrium state at rest with the molecular number density  $n_0$  and temperature  $T_0$  when gas B is absent (i.e.,  $l_0 = 1 / [\sqrt{2} \pi (d^A)^2 n_0]$ ). The  $x_i$  is the nondimensional coordinate system defined by  $x_i = X_i l_0^{-1} (\sqrt{\pi}/2)^{-1}$ . The  $(2kT_0/m^A)^{1/2} \zeta_i$  [or  $(2kT_0/m^A)^{1/2} \boldsymbol{\zeta}$ ] is the molecular velocity,  $n_0 (2kT_0/m^A)^{-3/2} (X_0^\alpha + \phi^\alpha) E^\alpha$  is the velocity distribution function of the molecules of gas  $\alpha$ , where  $E^\alpha(\boldsymbol{\zeta}) = (\hat{m}^\alpha/\pi)^{3/2} \exp(-\hat{m}^\alpha |\boldsymbol{\zeta}|^2)$  with  $\hat{m}^\alpha = m^\alpha/m^A$ , and  $\hat{d}^\alpha = d^\alpha/d^A$ . The molecular number density, density, pressure, temperature, flow velocity, stress tensor, and heat-flow vector of gas  $\alpha$  are denoted, respectively, by  $n_0(X_0^\alpha + N^\alpha)$ ,  $n_0 m^A (\hat{m}^\alpha X_0^\alpha + \omega^\alpha)$ ,  $p_0(X_0^\alpha + P^\alpha)$ ,  $T_0(1 + \tau^\alpha)$ ,  $(2kT_0/m^A)^{1/2} u_i^\alpha$ ,  $p_0(X_0^\alpha \delta_{ij} + P_{ij}^\alpha)$ , and  $p_0(2kT_0/m^A)^{1/2} Q_i^\alpha$ , where  $\delta_{ij}$  is Kronecker's delta. Those of the mixture are denoted by  $n_0(1 + N)$ ,  $n_0 m^A (\sum_{\beta=A,B} \hat{m}^\beta X_0^\beta + \omega)$ ,  $p_0(1 + P)$ ,  $T_0(1 + \tau)$ ,  $(2kT_0/m^A)^{1/2} u_i$ ,  $p_0(\delta_{ij} + P_{ij})$ , and  $p_0(2kT_0/m^A)^{1/2} Q_i$ .

The linearized Boltzmann equation in the present case ( $\partial/\partial t = \partial/\partial x_3 = 0$ ) is written as<sup>41–43</sup>

$$\zeta_1 \frac{\partial \phi^\alpha}{\partial x_1} + \zeta_2 \frac{\partial \phi^\alpha}{\partial x_2} = \sum_{\beta=A,B} K^{\beta\alpha} \tilde{L}^{\beta\alpha}(X_0^\alpha \phi^\beta, X_0^\beta \phi^\alpha), \quad (1)$$

where  $\tilde{L}^{\beta\alpha}$  is the linearized collision integral defined by

$$\begin{aligned} \tilde{L}^{\beta\alpha}(f, g) = & \frac{1}{4\sqrt{2\pi}} \int [f(\zeta'_*) - f(\zeta_*) + g(\zeta') - g(\zeta)] \\ & \times E^\beta(\zeta'_*) |\mathbf{e} \cdot \hat{\mathbf{V}}| d\Omega(\mathbf{e}) d^3 \zeta_*, \end{aligned} \quad (2)$$

with

$$\zeta' = \zeta + \frac{\hat{\mu}^{\beta\alpha}}{\hat{m}^\alpha} (\mathbf{e} \cdot \hat{\mathbf{V}}) \mathbf{e}, \quad \zeta'_* = \zeta_* - \frac{\hat{\mu}^{\beta\alpha}}{\hat{m}^\beta} (\mathbf{e} \cdot \hat{\mathbf{V}}) \mathbf{e}, \quad (3a)$$

$$\hat{\mathbf{V}} = \zeta_* - \zeta, \quad d^3 \zeta_* = d\zeta_{*1} d\zeta_{*2} d\zeta_{*3}, \quad (3b)$$

$$K^{\beta\alpha} = \left( \frac{\hat{\mu}^\alpha + \hat{\mu}^\beta}{2} \right)^2, \quad \hat{\mu}^{\beta\alpha} = \frac{2\hat{m}^\alpha \hat{m}^\beta}{\hat{m}^\alpha + \hat{m}^\beta}. \quad (3c)$$

Here  $\mathbf{e}$  is a unit vector,  $\zeta_*$  the variable of integration corresponding to  $\zeta$ , and  $d\Omega(\mathbf{e})$  the solid angle element in the direction of  $\mathbf{e}$ . The integration in Eq. (2) is carried out over the whole space of  $\zeta_*$  and over the all directions of  $\mathbf{e}$ .

The diffuse reflection condition on the wall ( $x_1=0$ ) is written as

$$\begin{aligned} \phi^\alpha = c_I X_0^\alpha (\hat{m}^\alpha \zeta_j^2 - 2)x_2 - 2(\pi \hat{m}^\alpha)^{1/2} \int_{\zeta_1 < 0} \zeta_1 \phi^\alpha E^\alpha d^3 \zeta, \\ \zeta_1 > 0, \end{aligned} \quad (4a)$$

for problem I (thermal slip), and

$$\phi^\alpha = -2(\pi \hat{m}^\alpha)^{1/2} \int_{\zeta_1 < 0} \zeta_1 \phi^\alpha E^\alpha d^3 \zeta, \quad \zeta_1 > 0, \quad (4b)$$

for problem II (diffusion slip). Here  $c_I$  is the dimensionless gradient of the wall temperature defined by

$$c_I = \frac{\sqrt{\pi}}{2} l_0 \frac{\tilde{C}_I}{T_0}.$$

Incidentally, for later use, we also define the dimensionless concentration gradient  $c_{II}$  of gas A away from the wall by

$$c_{II} = \frac{\sqrt{\pi}}{2} l_0 \tilde{C}_{II}^A.$$

The macroscopic variables  $N^\alpha$ ,  $\omega^\alpha$ ,  $u_i^\alpha$ , etc. of gas  $\alpha$  are written in terms of  $\phi^\alpha$  as

$$\begin{aligned} N^\alpha &= \int \phi^\alpha E^\alpha d^3 \zeta, \\ \omega^\alpha &= \hat{m}^\alpha \int \phi^\alpha E^\alpha d^3 \zeta (= \hat{m}^\alpha N^\alpha), \\ u_i^\alpha &= \frac{1}{X_0^\alpha} \int \zeta_i \phi^\alpha E^\alpha d^3 \zeta, \\ \tau^\alpha &= \frac{2}{3} \frac{1}{X_0^\alpha} \int \left( \hat{m}^\alpha \zeta_j^2 - \frac{3}{2} \right) \phi^\alpha E^\alpha d^3 \zeta, \end{aligned} \quad (5)$$

$$P^\alpha = \frac{2}{3} \hat{m}^\alpha \int \zeta_j^2 \phi^\alpha E^\alpha d^3 \zeta (= N^\alpha + X_0^\alpha \tau^\alpha),$$

$$P_{ij}^\alpha = 2\hat{m}^\alpha \int \zeta_i \zeta_j \phi^\alpha E^\alpha d^3 \zeta,$$

$$Q_i^\alpha = \hat{m}^\alpha \int \zeta_i \zeta_j^2 \phi^\alpha E^\alpha d^3 \zeta - \frac{5}{2} X_0^\alpha u_i^\alpha.$$

Here and henceforth, unless otherwise stated, the integration with respect to  $\zeta$  is performed over its whole space. The macroscopic variables of the mixture are expressed in terms of those of component gases as

$$\begin{aligned} N &= \sum_{\beta=A,B} N^\beta, \quad \omega = \sum_{\beta=A,B} \omega^\beta, \quad P = \sum_{\beta=A,B} P^\beta, \\ u_i &= \left( \sum_{\beta=A,B} \hat{m}^\beta X_0^\beta u_i^\beta \right) / \left( \sum_{\beta=A,B} \hat{m}^\beta X_0^\beta \right), \end{aligned} \quad (6)$$

$$\tau = \sum_{\beta=A,B} X_0^\beta \tau^\beta, \quad P_{ij} = \sum_{\beta=A,B} P_{ij}^\beta,$$

$$Q_i = \sum_{\beta=A,B} \left[ Q_i^\beta - \frac{5}{2} X_0^\beta (u_i - u_i^\beta) \right].$$

If we denote by  $(X_0^\alpha + \chi^\alpha)$  the concentration of gas  $\alpha$ ,  $\chi^\alpha$  is expressed as

$$\chi^\alpha = N^\alpha - X_0^\alpha N. \quad (7)$$

Note that  $\chi^A = -\chi^B$  because of the relations  $N = N^A + N^B$  and  $X_0^A + X_0^B = 1$ .

### III. PRELIMINARY ANALYSIS

#### A. Asymptotic solution away from the wall

Let us consider the function

$$\phi_{\text{asy}}^\alpha = X_0^\alpha \left[ \left( \hat{m}^\alpha \zeta^2 - \frac{5}{2} \right) x_2 + 2\hat{m}^\alpha b_I \zeta_2 - \zeta_2 A^\alpha(\zeta) \right], \quad (8a)$$

for problem I and

$$\begin{aligned} \phi_{\text{asy}}^\alpha = & (\delta_{\alpha A} - \delta_{\alpha B}) x_2 + 2\hat{m}^\alpha X_0^\alpha b_{II} \zeta_2 \\ & - X_0^\alpha \zeta_2 [D^{(A)\alpha}(\zeta) - D^{(B)\alpha}(\zeta)], \end{aligned} \quad (8b)$$

for problem II, where  $\zeta = |\boldsymbol{\zeta}| = \sqrt{\zeta_j^2}$ ,  $\delta_{AA} = \delta_{BB} = 1$  and  $\delta_{AB} = \delta_{BA} = 0$ . Here  $b_I$  and  $b_{II}$  are undetermined constants, and the functions  $A^\alpha$ ,  $D^{(A)\alpha}$ , and  $D^{(B)\alpha}$  are the solutions of the following integral equations:<sup>42-44</sup>

$$\sum_{\beta=A,B} K^{\beta\alpha} X_0^\beta \tilde{L}^{\beta\alpha}(\zeta_i A^\beta, \zeta_i A^\alpha) = -\zeta_i \left( \hat{m}^\alpha \zeta^2 - \frac{5}{2} \right), \quad (9a)$$

subsidiary condition:  $\sum_{\beta=A,B} \hat{m}^\beta X_0^\beta \int_0^\infty \zeta^4 A^\beta E^\beta d\zeta = 0,$

and

$$\begin{aligned} & \sum_{\beta=A,B} K^{\beta\alpha} X_0^\alpha X_0^\beta \tilde{L}^{\beta\alpha}(\zeta_i D^{(\gamma)\beta}, \zeta_i D^{(\gamma)\alpha}) \\ &= -\zeta_i \left( \delta_{\alpha\gamma} - \frac{\hat{m}^\alpha X_0^\alpha}{\sum_{\beta=A,B} \hat{m}^\beta X_0^\beta} \right), \end{aligned} \quad (9b)$$

subsidiary condition:

$$\sum_{\beta=A,B} \hat{m}^\beta X_0^\beta \int_0^\infty \zeta^4 D^{(\alpha)\beta} E^\beta d\zeta = 0.$$

The function  $\phi_{\text{asy}}^\alpha$  satisfies the Boltzmann equation (1). The corresponding macroscopic variables take the following form: for  $\phi_{\text{asy}}^\alpha$  in Eq. (8a),

$$\begin{aligned} N^\alpha &= -X_0^\alpha x_2, \quad \omega^\alpha = -\hat{m}^\alpha X_0^\alpha x_2, \\ \tau^\alpha &= x_2, \quad \chi^\alpha = P^\alpha = P_{ij}^\alpha = 0, \\ u_i^\alpha &= (b_I - \hat{D}_{T\alpha}) \delta_{i2}, \quad Q_i^\alpha = -\hat{\lambda}^{\alpha'} X_0^\alpha \delta_{i2}, \\ N &= -x_2, \quad \omega = -(\hat{m}^A X_0^A + \hat{m}^B X_0^B) x_2, \\ \tau &= x_2, \quad P = P_{ij} = 0, \quad u_i = b_I \delta_{i2}, \\ Q_i &= -\left[ \hat{\lambda}' + \frac{5}{2} (X_0^A \hat{D}_{TA} + X_0^B \hat{D}_{TB}) \right] \delta_{i2}, \end{aligned} \quad (10a)$$

and for  $\phi_{\text{asy}}^\alpha$  in Eq. (8b),

$$\begin{aligned} N^\alpha &= P^\alpha = \chi^\alpha = (\delta_{\alpha A} - \delta_{\alpha B}) x_2, \\ \omega^\alpha &= \hat{m}^\alpha (\delta_{\alpha A} - \delta_{\alpha B}) x_2, \quad \tau^\alpha = 0, \\ u_i^\alpha &= (b_{II} - \hat{\Delta}_{\alpha A} + \hat{\Delta}_{\alpha B}) \delta_{i2}, \\ P_{ij}^\alpha &= (\delta_{\alpha A} - \delta_{\alpha B}) x_2 \delta_{ij}, \\ Q_i^\alpha &= -X_0^\alpha (\hat{\Gamma}_D^{(A)\alpha} - \hat{\Gamma}_D^{(B)\alpha}) \delta_{i2}, \\ \omega &= (\hat{m}^A - \hat{m}^B) x_2, \\ N = P = \tau &= P_{ij} = 0, \quad u_i = b_{II} \delta_{i2}, \\ Q_i &= -\left[ (\hat{D}_{TA} - \hat{D}_{TB}) + \frac{5}{2} \sum_{\beta=A,B} X_0^\beta (\hat{\Delta}_{\beta A} - \hat{\Delta}_{\beta B}) \right] \delta_{i2}. \end{aligned} \quad (10b)$$

Here  $\hat{\lambda}^{\alpha'}$ ,  $\hat{\Delta}_{\alpha\beta}$ ,  $\hat{D}_{T\alpha}$ ,  $\hat{\Gamma}_D^{(\alpha)\beta}$ , and  $\hat{\lambda}'$  are functions of  $X_0^A$ ,  $\hat{m}^B$ , and  $\hat{d}^B$  and are related to the transport coefficients (see Appendix A).

It is seen from the form of  $P$ ,  $\tau$ , and  $\chi^\alpha$  in Eq. (10a) that  $\phi_{\text{asy}}^\alpha$  of (8a) multiplied by  $c_I$  is the solution describing the state at infinity of problem I. Similarly, it is seen from the form of  $P$ ,  $\tau$ , and  $\chi^\alpha$  in Eq. (10b) that  $\phi_{\text{asy}}^\alpha$  of (8b) multiplied by  $c_{II}$  is the solution describing the state at infinity of problem II.

The asymptotic solution  $c_I \phi_{\text{asy}}^\alpha$  or  $c_{II} \phi_{\text{asy}}^\alpha$  is seen to represent the state of the mixture described by the fluid-dynamic equation. Therefore we call  $c_I \phi_{\text{asy}}^\alpha$  or  $c_{II} \phi_{\text{asy}}^\alpha$  the fluid-dynamic solution.

## B. Knudsen-layer problems

Let us now seek the solution of problems I and II in the form

$$\phi^\alpha = c [\phi_{\text{asy}}^\alpha + \phi_K^\alpha(x_1, \zeta_i)], \quad (11)$$

where  $c = c_I$  for problem I and  $c = c_{II}$  for problem II. Substituting Eq. (11) into Eqs. (1) and (4a) or (4b) and taking into account that  $\phi_{\text{asy}}^\alpha$  satisfies the condition at infinity, we obtain the following equation and boundary condition for  $\phi_K^\alpha$ :

$$\zeta_1 \frac{\partial \phi_K^\alpha}{\partial x_1} = \sum_{\beta=A,B} K^{\beta\alpha} \tilde{L}^{\beta\alpha}(X_0^\alpha \phi_K^\beta, X_0^\beta \phi_K^\alpha), \quad (12)$$

$$\begin{aligned} \phi_K^\alpha &= -2\hat{m}^\alpha X_0^\alpha b_I \zeta_2 + X_0^\alpha \zeta_2 A^\alpha(\zeta) \\ &\quad - 2(\pi \hat{m}^\alpha)^{1/2} \int_{\zeta_1 < 0} \zeta_1 \phi_K^\alpha E^\alpha d^3 \zeta, \\ \zeta_1 > 0, \quad x_1 &= 0, \quad \text{for problem I,} \end{aligned} \quad (13a)$$

$$\begin{aligned} \phi_K^\alpha &= -2\hat{m}^\alpha X_0^\alpha b_{II} \zeta_2 + X_0^\alpha \zeta_2 [D^{(A)\alpha}(\zeta) - D^{(B)\alpha}(\zeta)] \\ &\quad - 2(\pi \hat{m}^\alpha)^{1/2} \int_{\zeta_1 < 0} \zeta_1 \phi_K^\alpha E^\alpha d^3 \zeta, \\ \zeta_1 > 0, \quad x_1 &= 0, \quad \text{for problem II,} \end{aligned} \quad (13b)$$

$$\phi_K^\alpha \rightarrow 0, \quad \text{as } x_1 \rightarrow \infty. \quad (14)$$

We call the half-space problem (12), (13a), and (14) the Knudsen-layer problem for the thermal slip and the problem (12), (13b), and (14) that for the diffusion slip. For each problem, there is a unique solution  $\phi_K^\alpha$  if and only if the constant  $b_I$  or  $b_{II}$  takes a special value, and  $\phi_K^\alpha$  decays exponentially as  $x_1 \rightarrow \infty$ . This is a consequence of the existence and uniqueness theorem for the Knudsen-layer problem for a binary mixture of hard-sphere gases, which was proved recently in Ref. 45. The theorem is the extension of that for a single-component gas first conjectured by Grad<sup>46</sup> and proved later for various molecular models.<sup>47-51</sup> In this way the constants  $b_I$  and  $b_{II}$  in the fluid-dynamic solutions,  $c_I \phi_{\text{asy}}^\alpha$  and  $c_{II} \phi_{\text{asy}}^\alpha$ , are determined by the analysis of the Knudsen-layer problem. It is seen from the expression of  $u_i$  in Eqs. (10a) and (10b) that  $b_I$  or  $b_{II}$  is the flow velocity of the mixture away from the wall when  $c_I = 1$  or  $c_{II} = 1$ .

Since  $\hat{m}^A = \hat{d}^A = 1$  and  $X_0^A + X_0^B = 1$ , both problems are characterized by the three parameters,

$$\hat{m}^B \text{ (or } m^B/m^A), \quad \hat{d}^B \text{ (or } d^B/d^A), \quad X_0^A.$$

Multiplying Eq. (12) by  $\hat{m}^\alpha \zeta_2 E^\alpha$  for  $\alpha = A, B$ , adding the resulting equations, and taking into account the condition (14), one obtains the relation

$$\sum_{\beta=A,B} \hat{m}^\beta \int \zeta_1 \zeta_2 \phi_K^\beta E^\beta d^3 \zeta = 0. \quad (15)$$

This is the momentum conservation law in the  $x_2$ -direction.

**C. Similarity solution and macroscopic variables**

Let us assume that  $\phi_K^\alpha$  is of the form

$$\phi_K^\alpha = (\zeta_2 / \zeta_\rho) \Phi^\alpha(x_1, \zeta_1, \zeta_\rho), \tag{16}$$

where  $\zeta_\rho = \sqrt{\zeta_2^2 + \zeta_3^2}$ . This  $\phi_K^\alpha$  is compatible with Eqs. (12)–(14), which can be seen by using the spherical symmetry<sup>4</sup> of the collision operator  $\tilde{L}^{\beta\alpha}$ . Therefore, using the notations

$$\Psi^\alpha(x_1, \zeta_1, \zeta_\rho) = \Phi^\alpha(x_1, \zeta_1, \zeta_\rho) E^\alpha, \tag{17a}$$

$$\tilde{L}^{\beta\alpha}(\Psi^\beta, \Psi^\alpha) = (\zeta_\rho / \zeta_2) \tilde{L}^{\beta\alpha} \left( \frac{\zeta_2}{\zeta_\rho} \Phi^\beta, \frac{\zeta_2}{\zeta_\rho} \Phi^\alpha \right) E^\alpha, \tag{17b}$$

we can transform the boundary-value problem (12)–(14) for  $\phi_K^\alpha$  into that for  $\Psi^\alpha$ :

$$\zeta_1 \frac{\partial \Psi^\alpha}{\partial x_1} = \sum_{\beta=A,B} K^{\beta\alpha} \tilde{L}^{\beta\alpha} (X_0^{\alpha\beta} \Psi^\beta, X_0^{\beta\alpha} \Psi^\alpha), \tag{18}$$

$$\Psi^\alpha = X_0^\alpha \zeta_\rho (-2\hat{m}^\alpha b_I + A^\alpha) E^\alpha, \tag{19a}$$

$$\zeta_1 > 0, \quad x_1 = 0, \quad \text{for problem I,}$$

$$\Psi^\alpha = X_0^\alpha \zeta_\rho (-2\hat{m}^\alpha b_{II} + D^{(A)\alpha} - D^{(B)\alpha}) E^\alpha, \tag{19b}$$

$$\zeta_1 > 0, \quad x_1 = 0, \quad \text{for problem II,}$$

$$\Psi^\alpha \rightarrow 0, \quad \text{as } x_1 \rightarrow \infty. \tag{20}$$

Note that  $E^\alpha$ ,  $A^\alpha$ , and  $D^{(B)\alpha}$  are now the functions of  $\zeta_1$  and  $\zeta_\rho$  because  $\zeta = |\boldsymbol{\zeta}| = (\zeta_1^2 + \zeta_\rho^2)^{1/2}$ . Following the transformation by Grad<sup>52</sup> for a single-component gas, one can derive the expression of  $\tilde{L}^{\beta\alpha}$  in terms of integral kernels. That is,

$$\tilde{L}^{\beta\alpha}(f, g) = \tilde{L}_1^{\beta\alpha}(f) + \tilde{L}_2^{\beta\alpha}(g) - \tilde{L}_3^{\beta\alpha}(f) - \nu^\beta(\zeta) g, \tag{21}$$

with

$$\tilde{L}_J^{\beta\alpha}(f) = E^\alpha \int_0^\infty d\xi_\rho \int_{-\infty}^\infty d\xi_1 \mathcal{K}_J^{\beta\alpha}(\xi_1, \xi_\rho, \zeta_1, \zeta_\rho) \times f(\xi_1, \xi_\rho) \quad (J=1,2,3), \tag{22}$$

$$\nu^\alpha(\zeta) = \frac{1}{2\sqrt{2}} \left( \frac{1}{\sqrt{\hat{m}^\alpha}} \exp(-\hat{m}^\alpha \zeta^2) + \left( 2\zeta + \frac{1}{\hat{m}^\alpha \zeta} \right) \int_0^{\sqrt{\hat{m}^\alpha} \zeta} \exp(-y^2) dy \right). \tag{23}$$

The explicit form of integral kernels  $\mathcal{K}_J^{\beta\alpha}$  ( $J=1,2,3$ ) is given in Appendix B.

Substituting Eq. (11) with the similarity solution (16) [and (17a)] into Eqs. (5)–(7), we have the following expression for the macroscopic variables: for problem I,

$$N^\alpha = -c_I X_0^\alpha x_2, \quad \omega^\alpha = -c_I \hat{m}^\alpha X_0^\alpha x_2, \tag{24a}$$

$$\tau^\alpha = c_I x_2, \quad \chi^\alpha = P^\alpha = 0,$$

$$u_i^\alpha = c_I (b_I - \hat{D}_{T\alpha} + U^\alpha) \delta_{i2},$$

$$P_{ij}^\alpha = c_I S^\alpha (\delta_{i1} \delta_{j2} + \delta_{i2} \delta_{j1}),$$

$$Q_i^\alpha = c_I (-\hat{\lambda}^{\alpha'} X_0^\alpha + H^\alpha) \delta_{i2}, \tag{24b}$$

$$N = -c_I x_2, \quad \omega = -c_I (\hat{m}^A X_0^A + \hat{m}^B X_0^B) x_2,$$

$$u_i = c_I (b_I + U) \delta_{i2}, \quad \tau = c_I x_2, \quad P = 0,$$

$$P_{ij} = c_I (S^A + S^B) (\delta_{i1} \delta_{j2} + \delta_{i2} \delta_{j1}),$$

$$Q_i = c_I \left( -\hat{\lambda}' - \frac{5}{2} (X_0^A \hat{D}_{TA} + X_0^B \hat{D}_{TB}) + H \right) \delta_{i2},$$

and for problem II,

$$N^\alpha = P^\alpha = \chi^\alpha = c_{II} (\delta_{\alpha A} - \delta_{\alpha B}) x_2,$$

$$\omega^\alpha = c_{II} \hat{m}^\alpha (\delta_{\alpha A} - \delta_{\alpha B}) x_2, \quad \tau^\alpha = 0,$$

$$u_i^\alpha = c_{II} (b_{II} - \hat{\Delta}_{\alpha A} + \hat{\Delta}_{\alpha B} + U^\alpha) \delta_{i2},$$

$$P_{ij}^\alpha = c_{II} [(\delta_{\alpha A} - \delta_{\alpha B}) x_2 \delta_{ij} + S^\alpha (\delta_{i1} \delta_{j2} + \delta_{i2} \delta_{j1})],$$

$$Q_i^\alpha = c_{II} [-X_0^\alpha (\hat{\Gamma}_D^{(A)\alpha} - \hat{\Gamma}_D^{(B)\alpha}) + H^\alpha] \delta_{i2}, \tag{24c}$$

$$N = P = \tau = 0, \quad \omega = c_{II} (\hat{m}^A - \hat{m}^B) x_2,$$

$$u_i = c_{II} (b_{II} + U) \delta_{i2},$$

$$P_{ij} = c_{II} (S^A + S^B) (\delta_{i1} \delta_{j2} + \delta_{i2} \delta_{j1}),$$

$$Q_i = c_{II} \left( -(\hat{D}_{TA} - \hat{D}_{TB}) - \frac{5}{2} \sum_{\beta=A,B} X_0^\beta (\hat{\Delta}_{\beta A} - \hat{\Delta}_{\beta B}) + H \right) \delta_{i2},$$

where

$$U^\alpha(x_1) = \frac{\pi}{X_0^\alpha} \int_0^\infty \int_{-\infty}^\infty \zeta_\rho^2 \Psi^\alpha d\zeta_1 d\zeta_\rho, \tag{25a}$$

$$U(x_1) = \left( \sum_{\beta=A,B} \hat{m}^\beta X_0^\beta U^\beta \right) / \left( \sum_{\beta=A,B} \hat{m}^\beta X_0^\beta \right), \tag{25b}$$

$$S^\alpha(x_1) = 2\pi \hat{m}^\alpha \int_0^\infty \int_{-\infty}^\infty \zeta_1 \zeta_\rho^2 \Psi^\alpha d\zeta_1 d\zeta_\rho, \tag{25c}$$

$$H^\alpha(x_1) = \pi \int_0^\infty \int_{-\infty}^\infty \zeta_\rho^2 \left( \hat{m}^\alpha (\zeta_1^2 + \zeta_\rho^2) - \frac{5}{2} \right) \Psi^\alpha d\zeta_1 d\zeta_\rho, \tag{25d}$$

$$H(x_1) = \sum_{\beta=A,B} \left( H^\beta + \frac{5}{2} X_0^\beta (U^\beta - U) \right). \tag{25e}$$

The functions  $U^\alpha$ ,  $U$ ,  $S^\alpha$ ,  $H^\alpha$ , and  $H$ , which we call the Knudsen-layer functions, decay exponentially as  $x_1 \rightarrow \infty$ . In Eqs. (24a) and (24b), they appear only in the  $x_2$ -component of flow velocities  $u_2^\alpha$  and  $u_2$ , in that of heat-flow vectors  $Q_2^\alpha$  and  $Q_2$ , and in the  $x_1 x_2$ -component of stress tensors  $P_{12}^\alpha$  (or  $P_{21}^\alpha$ ) and  $P_{12}$  (or  $P_{21}$ ). On the other hand, from the relation (15) we find

$$S^A + S^B = 0, \tag{26}$$

so that the Knudsen-layer function does not appear in the stress tensor  $P_{ij}$  of the mixture. The property (26) is used as a measure of accuracy of the numerical solution later. In

summary, except  $u_2^\alpha$ ,  $u_2$ ,  $Q_2^\alpha$ ,  $Q_2$ , and  $P_{12}^\alpha$  (or  $P_{21}^\alpha$ ), the macroscopic variables are expressed only by the fluid-dynamic solution: Eq. (10a) multiplied by  $c_I$  or Eq. (10b) by  $c_{II}$ .

As is mentioned in Sec. III B,  $b_I c_I$  and  $b_{II} c_{II}$  are the flow velocity of the mixture away from the wall. On the other hand, the expression of  $u_i$  in Eqs. (24a) and (24b) shows that, if the Knudsen-layer function is neglected, the flow velocity of the mixture on the wall ( $x_1=0$ ) is also given by

$$\begin{aligned} u_2 &= b_I c_I = b_I \left( \frac{d\tau}{dx_2} \right), \quad \text{for problem I,} \\ u_2 &= b_{II} c_{II} = b_{II} \left( \frac{d\chi^A}{dx_2} \right), \quad \text{for problem II.} \end{aligned} \quad (27)$$

This means that the flow velocity of the fluid-dynamic solution is subject to the slip on the wall caused by the temperature or concentration gradient. From this point of view, the constant  $b_I$  is called the coefficient of thermal slip and  $b_{II}$  the coefficient of diffusion slip.

## IV. NUMERICAL ANALYSIS

### A. Plan of computation

As is mentioned in the first paragraph in Sec. III B, the reduced boundary-value problem (18)–(20) has a solution if and only if the undetermined constant  $b$  takes a special value, where  $b = b_I$  for problem I and  $b = b_{II}$  for problem II. A straightforward way to solve the problem is to repeat computation with different  $b$  until a solution satisfying the condition (20) is obtained. However, since such a method is generally inefficient, we adopt the method devised in Ref. 12.

Consider the function

$$\tilde{\Psi}^\alpha(x_1, \zeta_1, \zeta_\rho) = \Psi^\alpha(x_1, \zeta_1, \zeta_\rho) + 2\hat{m}^\alpha X_0^\alpha \delta \zeta_\rho E^\alpha, \quad (28)$$

where  $\delta$  is an undetermined constant. Since the second term on the right is a solution of Eq. (18),  $\tilde{\Psi}^\alpha$  also satisfies Eq. (18):

$$\zeta_1 \frac{\partial \tilde{\Psi}^\alpha}{\partial x_1} = \sum_{\beta=A,B} K^{\beta\alpha} \tilde{\mathcal{L}}^{\beta\alpha} (X_0^\alpha \tilde{\Psi}^\beta, X_0^\beta \tilde{\Psi}^\alpha). \quad (29)$$

The boundary condition for  $\tilde{\Psi}^\alpha$  on the wall is obtained from Eqs. (19a) and (19b) with (28) as

$$\begin{aligned} \tilde{\Psi}^\alpha &= X_0^\alpha \zeta_\rho (-2\hat{m}^\alpha b_{I*} + A^\alpha) E^\alpha, \\ \zeta_1 &> 0, \quad x_1 = 0, \quad \text{for problem I,} \end{aligned} \quad (30a)$$

$$\begin{aligned} \tilde{\Psi}^\alpha &= X_0^\alpha \zeta_\rho (-2\hat{m}^\alpha b_{II*} + D^{(A)\alpha} - D^{(B)\alpha}) E^\alpha, \\ \zeta_1 &> 0, \quad x_1 = 0, \quad \text{for problem II,} \end{aligned} \quad (30b)$$

where

$$b_{I*} = b_I - \delta, \quad b_{II*} = b_{II} - \delta. \quad (31)$$

Since  $\Psi^\alpha$  decays exponentially (see the first paragraph in Sec. III B), it is negligible at a distance large enough, say at  $x_1 = d$ . Consequently  $\tilde{\Psi}^\alpha$  at  $x_1 = d$  can be written as

$$\tilde{\Psi}^\alpha(d, \zeta_1, \zeta_\rho) = 2\hat{m}^\alpha X_0^\alpha \delta \zeta_\rho E^\alpha. \quad (32)$$

The corresponding flow velocity  $\tilde{U}(x_1)$  of the mixture, which is defined by Eq. (25b) [with (25a)] with  $\Psi^\alpha$  replaced by  $\tilde{\Psi}^\alpha$ , takes the value  $\delta$ :

$$\tilde{U}(d) = \delta. \quad (33)$$

Because of Eq. (32),  $\tilde{\Psi}^\alpha$  satisfies the reflection condition at  $x_1 = d$ :

$$\tilde{\Psi}^\alpha(d, \zeta_1, \zeta_\rho) = \tilde{\Psi}^\alpha(d, -\zeta_1, \zeta_\rho). \quad (34)$$

We solve the boundary-value problem (29), (30a) [or (30b)], and (34) for a given  $b_{I*}$  (or  $b_{II*}$ ), instead of solving the original problem (18)–(20) directly. Once  $\tilde{\Psi}^\alpha$  is obtained,  $\delta$  is determined by Eq. (33). Then,  $\Psi^\alpha$  and  $b_I$  (or  $b_{II}$ ) are obtained from Eqs. (28) and (31).

### B. Finite-difference scheme

Because of the factor  $E^\alpha$  [see Eqs. (16) and (28)],  $\tilde{\Psi}^\alpha$  is expected to decay rapidly as  $|\zeta_1|$  or  $\zeta_\rho$  tends to  $\infty$ . Thus in the actual computation we restrict the regions of  $\zeta_1$  and  $\zeta_\rho$  to finite ones. That is, for a proper choice of  $Z_1^\alpha (>0)$  and  $Z_\rho^\alpha (>0)$ , we carry out the numerical computation for  $\tilde{\Psi}^\alpha$  in the region  $0 \leq x_1 \leq d$ ,  $-Z_1^\alpha \leq \zeta_1 \leq Z_1^\alpha$ , and  $0 \leq \zeta_\rho \leq Z_\rho^\alpha$ . The regions of  $x_1$ ,  $\zeta_1$ , and  $\zeta_\rho$  are divided into  $N_x$ ,  $4N_1$ , and  $2N_\rho$  intervals in the following way:

$$\begin{aligned} 0 &= x_1^{(0)} < x_1^{(1)} < \dots < x_1^{(N_x)} = d, \\ -Z_1^\alpha &= \zeta_1^{\alpha(-2N_1)} < \zeta_1^{\alpha(-2N_1+1)} < \dots < \zeta_1^{\alpha(0)} (= 0) \\ &< \zeta_1^{\alpha(1)} < \dots < \zeta_1^{\alpha(2N_1)} = Z_1^\alpha, \\ 0 &= \zeta_\rho^{\alpha(0)} < \zeta_\rho^{\alpha(1)} < \dots < \zeta_\rho^{\alpha(2N_\rho)} = Z_\rho^\alpha. \end{aligned}$$

Here  $Z_1^\alpha$  and  $Z_\rho^\alpha$  are taken to be  $Z_1^\alpha = Z_1 / \sqrt{\hat{m}^\alpha}$  and  $Z_\rho^\alpha = Z_\rho / \sqrt{\hat{m}^\alpha}$  with  $Z_1$  and  $Z_\rho$  being constants common to  $\tilde{\Psi}^A$  and  $\tilde{\Psi}^B$  (see Table XII in Sec. VI). For later convenience, chiefly for the computation of collision integrals, the lattice points of  $\zeta_1$  are chosen to be symmetric with respect to  $\zeta_1 = 0$ , i.e.,  $\zeta_1^{\alpha(j)} = -\zeta_1^{\alpha(-j)}$ . We denote the value of a physical quantity at a lattice point by attaching the subscript label corresponding to the point, e.g.,  $\tilde{\Psi}_{(i,j,k)}^\alpha = \tilde{\Psi}^\alpha(x_1^{(i)}, \zeta_1^{\alpha(j)}, \zeta_\rho^{\alpha(k)})$ . For steady and spatially one-dimensional problems, it is known that the velocity distribution function is, in general, discontinuous at  $\zeta_1 = 0$  on the wall ( $x_1 = 0$ ) (see, for instance, Ref. 53). Thus  $\tilde{\Psi}^\alpha$  has two limiting values  $\tilde{\Psi}^\alpha(0, \pm 0, \zeta_\rho)$  on the wall. Taking it into account, we prepare two sets of values  $\tilde{\Psi}_{(0, \pm 0, k)}^\alpha$  for the lattice point  $(0, 0, \zeta_\rho^{\alpha(k)})$  in the computation.

We obtain the discrete solution  $\tilde{\Psi}_{(i,j,k)}^\alpha$  as the limit of the sequence  $\{\tilde{\Psi}_{(i,j,k)}^{\alpha(n)}\}$  ( $n=0, 1, 2, \dots$ ) constructed by the iteration using the following finite-difference scheme for Eq. (29):

$$\zeta_1^{\alpha(j)} \nabla_{ijk} \tilde{\Psi}^{\alpha(n+1)} = -\tilde{v}_{(j,k)}^\alpha \tilde{\Psi}_{(i,j,k)}^{\alpha(n+1)} + C_{(i,j,k)}^{\alpha(n)}, \quad (35)$$

where  $\nabla_{ijk}$  corresponds to  $\partial/\partial x_1$ , and  $\tilde{v}_{(j,k)}^\alpha$  and  $C_{(i,j,k)}^{\alpha(n)}$  are defined as

$$\tilde{v}_{(j,k)}^\alpha = K^{AA} X_0^A \nu^A(\zeta_1^{\alpha(j)}, \zeta_\rho^{\alpha(k)}) + K^{BA} X_0^B \nu^B(\zeta_1^{\alpha(j)}, \zeta_\rho^{\alpha(k)}), \quad (36a)$$

$$\begin{aligned} C_{(i,j,k)}^{A(n)} &= [K^{AA} X_0^A (\tilde{\mathcal{L}}_1^{AA} + \tilde{\mathcal{L}}_2^{AA} - \tilde{\mathcal{L}}_3^{AA}) \\ &\quad + K^{BA} X_0^B \tilde{\mathcal{L}}_2^{BA}] (\tilde{\Psi}^{A(n)})_{(i,j,k)} \\ &\quad + K^{BA} X_0^A (\tilde{\mathcal{L}}_1^{BA} - \tilde{\mathcal{L}}_3^{BA}) (\tilde{\Psi}^{B(n)})_{(i,j,k)}, \end{aligned} \quad (36b)$$

$$\begin{aligned} C_{(i,j,k)}^{B(n)} &= [K^{BB} X_0^B (\tilde{\mathcal{L}}_1^{BB} + \tilde{\mathcal{L}}_2^{BB} - \tilde{\mathcal{L}}_3^{BB}) \\ &\quad + K^{AB} X_0^A \tilde{\mathcal{L}}_2^{AB}] (\tilde{\Psi}^{B(n)})_{(i,j,k)} \\ &\quad + K^{AB} X_0^B (\tilde{\mathcal{L}}_1^{AB} - \tilde{\mathcal{L}}_3^{AB}) (\tilde{\Psi}^{A(n)})_{(i,j,k)}. \end{aligned} \quad (36c)$$

For  $\nabla_{ijk}$ , the following formulas are used: for  $1 \leq j \leq 2N_1$ ,

$$\nabla_{ijk} \tilde{\Psi}^{\alpha(n)} = \begin{cases} (\tilde{\Psi}_{(1,j,k)}^{\alpha(n)} - \tilde{\Psi}_{(0,j,k)}^{\alpha(n)})/h_1 & (i=1), \\ w_0(h_{i-1}, h_i) \tilde{\Psi}_{(i,j,k)}^{\alpha(n)} - w_1(h_{i-1}, h_i) \tilde{\Psi}_{(i-1,j,k)}^{\alpha(n)} \\ \quad + w_2(h_{i-1}, h_i) \tilde{\Psi}_{(i-2,j,k)}^{\alpha(n)} & (2 \leq i \leq N_x), \end{cases} \quad (37a)$$

and for  $-2N_1 \leq j \leq 0$ ,

$$\nabla_{ijk} \tilde{\Psi}^{\alpha(n)} = \begin{cases} \left( 2\tilde{\Psi}_{(N_x,j,k)}^{\alpha(n)} - \frac{3}{2}\tilde{\Psi}_{(N_x-1,j,k)}^{\alpha(n)} - \frac{1}{2}\tilde{\Psi}_{(N_x-1,-j,k)}^{\alpha(n)} \right) / h_{N_x} & (i=N_x-1), \\ -w_2(h_{i+2}, h_{i+1}) \tilde{\Psi}_{(i+2,j,k)}^{\alpha(n)} + w_1(h_{i+2}, h_{i+1}) \tilde{\Psi}_{(i+1,j,k)}^{\alpha(n)} - w_0(h_{i+2}, h_{i+1}) \tilde{\Psi}_{(i,j,k)}^{\alpha(n)} & (0 \leq i \leq N_x-2), \end{cases} \quad (37b)$$

where

$$\begin{aligned} h_i &= x_1^{(i)} - x_1^{(i-1)}, \quad w_0(a,b) = \frac{a+2b}{b(a+b)}, \\ w_1(a,b) &= \frac{a+b}{ab}, \quad w_2(a,b) = \frac{b}{a(a+b)}. \end{aligned} \quad (38)$$

The terms  $C_{(i,j,k)}^{\alpha(n)}$  are computed by the numerical kernel method first proposed in Ref. 11 for a single-component gas. The details of the method is given in Sec. IV C. The functions  $A^\alpha$  and  $D^{(\beta)\alpha}$ , which are the solutions of Eqs. (9a) and (9b), appear in the boundary conditions (30a) and (30b). In the present work, we use their accurate numerical data obtained in Ref. 44 for arbitrary values of  $X_0^A$  for a binary mixture of hard-sphere gases.

The solution procedure is as follows. Start with appropriate initial data  $\tilde{\Psi}_{(i,j,k)}^{\alpha(0)}$  and  $b_*$ . Suppose that  $\tilde{\Psi}_{(i,j,k)}^{\alpha(n)}$  is known. Then  $\tilde{\Psi}_{(i,j,k)}^{\alpha(n+1)}$  is computed by the following process.

- (i) Compute  $C_{(i,j,k)}^{\alpha(n)}$  using  $\tilde{\Psi}_{(i,j,k)}^{A(n)}$  and  $\tilde{\Psi}_{(i,j,k)}^{B(n)}$ .
- (ii) Using the boundary condition (30a) [or (30b)], compute  $\tilde{\Psi}_{(i,j,k)}^{\alpha(n+1)}$  ( $1 \leq j \leq 2N_1$ ) from  $i=1$  to  $N_x$  successively by Eq. (35) with (37a).
- (iii) Compute  $\tilde{\Psi}_{(N_x,j,k)}^{\alpha(n+1)}$  ( $-1 \geq j \geq -2N_1$ ) using the boundary condition (34). Since the lattice points of  $\zeta_1$  is symmetric with respect to  $\zeta_1=0$ ,  $\tilde{\Psi}_{(N_x,j,k)}^{\alpha(n+1)}$  is given by  $\tilde{\Psi}_{(N_x,j,k)}^{\alpha(n+1)} = \tilde{\Psi}_{(N_x,-j,k)}^{\alpha(n+1)}$ .
- (iv) Compute  $\tilde{\Psi}_{(i,j,k)}^{\alpha(n+1)}$  ( $-1 \geq j \geq -2N_1$ ) from  $i=N_x-1$  to 0 successively by Eq. (35) with (37b), using the data  $\tilde{\Psi}_{(N_x,j,k)}^{\alpha(n+1)}$  obtained in (iii).
- (v) Compute  $\tilde{\Psi}_{(0,-0,k)}^{\alpha(n+1)}$  and  $\tilde{\Psi}_{(i,0,k)}^{\alpha(n+1)}$  ( $i=1, \dots, N_x$ ) by Eq. (35) with  $\zeta_1^{(j)}=0$ . Compute  $\tilde{\Psi}_{(0,+0,k)}^{\alpha(n+1)}$  by the boundary condition (30a) [or (30b)].

We repeat steps (i)–(v) for  $n=0,1,2, \dots$ , until  $\tilde{\Psi}_{(i,j,k)}^{\alpha(n)}$  converges. Then  $\Psi_{(i,j,k)}^\alpha$  and  $b$  are obtained by Eqs. (28) and (31) with Eq. (33). The Knudsen-layer functions are obtained from the (discrete) solution by the integrations [Eqs. (25a)–(25d)] using Simpson's formula.

In the actual computation, we repeat the above process with new  $b$  as  $b_*$  in order to reduce the errors coming from the second term on the right-hand side of Eq. (28).

## C. Numerical kernel method

In order to obtain  $C_{(i,j,k)}^{\alpha(n)}$ , we have to carry out the complicated five-fold integrations numerically, which requires heavy computation. In Ref. 11, an accurate and efficient method for the computation of collision integrals was proposed for a single-component gas. We apply this method to the computation of  $C_{(i,j,k)}^{\alpha(n)}$ . We first introduce the following piecewise quadratic functions  $B_{l,m}^{\alpha\pm}(\zeta_1, \zeta_\rho)$  of  $\zeta_1$  and  $\zeta_\rho$ , localized around the lattice point  $(\zeta_1^{(l)}, \zeta_\rho^{(m)})$ :

$$B_{l,m}^{\alpha\pm}(\zeta_1, \zeta_\rho) = Y_l^{\alpha\zeta_1}(\zeta_1) \chi_{[0, z_1^\alpha]}(\pm \zeta_1) Y_m^{\alpha\zeta_\rho}(\zeta_\rho) \chi_{[0, z_\rho^\alpha]}(\zeta_\rho), \quad (39)$$

where  $Y_l^{\alpha z}(y)$  with  $y = \zeta_1, \zeta_\rho$  and  $z = \zeta_1, \zeta_\rho$  are defined by

$$Y_{2m}^{\alpha z}(y) = \begin{cases} \frac{(y-z^{\alpha(2m+2)})(y-z^{\alpha(2m+1)})}{(z^{\alpha(2m)}-z^{\alpha(2m+2)})(z^{\alpha(2m)}-z^{\alpha(2m+1)})}, & \text{for } z^{\alpha(2m)} < y < z^{\alpha(2m+2)}, \\ \frac{(y-z^{\alpha(2m-2)})(y-z^{\alpha(2m-1)})}{(z^{\alpha(2m)}-z^{\alpha(2m-2)})(z^{\alpha(2m)}-z^{\alpha(2m-1)})}, & \text{for } z^{\alpha(2m-2)} < y < z^{\alpha(2m)}, \\ 0, & \text{otherwise,} \end{cases} \quad (40a)$$

$$Y_{2m+1}^{\alpha z}(y) = \begin{cases} \frac{(y-z^{\alpha(2m+2)})(y-z^{\alpha(2m)})}{(z^{\alpha(2m+1)}-z^{\alpha(2m+2)})(z^{\alpha(2m+1)}-z^{\alpha(2m)})}, \\ \text{for } z^{\alpha(2m)} < y < z^{\alpha(2m+2)}, \\ 0, \text{ otherwise.} \end{cases} \quad (40b)$$

In Eq. (39),  $\chi_{[a,b]}(y)$  denotes the characteristic function of the interval  $[a,b]$ , i.e.,  $\chi_{[a,b]}(y)=1$  for  $a \leq y \leq b$  and  $\chi_{[a,b]}(y)=0$  otherwise. Then we expand  $\tilde{\Psi}^{\alpha(n)}$  at  $x_1 = x_1^{(i)}$  in terms of  $B_{l,m}^{\alpha \pm}(\zeta_1, \zeta_\rho)$  as follows:

$$\tilde{\Psi}^{\alpha(n)}(x_1^{(i)}, \zeta_1, \zeta_\rho) = \sum_{m=0}^{2N_\rho} \sum_{l=0}^{2N_1} (\tilde{\Psi}_{(i,l,m)}^{\alpha(n)} B_{l,m}^{\alpha+}(\zeta_1, \zeta_\rho) + \tilde{\Psi}_{(i,-l,m)}^{\alpha(n)} B_{-l,m}^{\alpha-}(\zeta_1, \zeta_\rho)). \quad (41)$$

In the above expression and in Eqs. (42a) and (42b) below, the  $\tilde{\Psi}_{(i,l,m)}^{\alpha(n)}$  and  $\tilde{\Psi}_{(i,-l,m)}^{\alpha(n)}$  for  $i=l=0$  should be regarded as  $\tilde{\Psi}_{(0,+0,m)}^{\alpha(n)}$  and  $\tilde{\Psi}_{(0,-0,m)}^{\alpha(n)}$  because  $\tilde{\Psi}^{\alpha}$  is discontinuous at  $\zeta_1 = 0$  on the wall. The substitution of Eq. (41) into Eqs. (36b) and (36c) gives the following expression for  $C_{(i,j,k)}^{\alpha(n)}$ :

$$C_{(i,j,k)}^{A(n)} = \sum_{m=0}^{2N_\rho} \sum_{l=0}^{2N_1} (C_{j,k,l,m}^{AA+} \tilde{\Psi}_{(i,l,m)}^{A(n)} + C_{j,k,l,m}^{BA+} \tilde{\Psi}_{(i,l,m)}^{B(n)} + C_{j,k,-l,m}^{AA-} \tilde{\Psi}_{(i,-l,m)}^{A(n)} + C_{j,k,-l,m}^{BA-} \tilde{\Psi}_{(i,-l,m)}^{B(n)}), \quad (42a)$$

$$C_{(i,j,k)}^{B(n)} = \sum_{m=0}^{2N_\rho} \sum_{l=0}^{2N_1} (C_{j,k,l,m}^{AB+} \tilde{\Psi}_{(i,l,m)}^{A(n)} + C_{j,k,l,m}^{BB+} \tilde{\Psi}_{(i,l,m)}^{B(n)} + C_{j,k,-l,m}^{AB-} \tilde{\Psi}_{(i,-l,m)}^{A(n)} + C_{j,k,-l,m}^{BB-} \tilde{\Psi}_{(i,-l,m)}^{B(n)}), \quad (42b)$$

where

$$C_{j,k,l,m}^{AA\pm} = [K^{AA} X_0^A (\tilde{\mathcal{L}}_1^{AA} + \tilde{\mathcal{L}}_2^{AA} - \tilde{\mathcal{L}}_3^{AA}) + K^{BA} X_0^B \tilde{\mathcal{L}}_2^{BA}] (B_{l,m}^{\alpha \pm})_{(j,k)}, \quad (43a)$$

$$C_{j,k,l,m}^{BA\pm} = K^{BA} X_0^A (\tilde{\mathcal{L}}_1^{BA} - \tilde{\mathcal{L}}_3^{BA}) (B_{l,m}^{\alpha \pm})_{(j,k)}, \quad (43b)$$

$$C_{j,k,l,m}^{AB\pm} = K^{AB} X_0^B (\tilde{\mathcal{L}}_1^{AB} - \tilde{\mathcal{L}}_3^{AB}) (B_{l,m}^{\alpha \pm})_{(j,k)}, \quad (43c)$$

$$C_{j,k,l,m}^{BB\pm} = [K^{BB} X_0^B (\tilde{\mathcal{L}}_1^{BB} + \tilde{\mathcal{L}}_2^{BB} - \tilde{\mathcal{L}}_3^{BB}) + K^{AB} X_0^A \tilde{\mathcal{L}}_2^{AB}] (B_{l,m}^{\alpha \pm})_{(j,k)}. \quad (43d)$$

We call  $C_{j,k,l,m}^{A\alpha\pm}$  and  $C_{j,k,l,m}^{B\alpha\pm}$  the numerical kernels of  $C_{(i,j,k)}^{\alpha(n)}$ . Note that  $C_{j,k,l,m}^{\beta\alpha\pm}(\alpha, \beta = A, B)$  is the integral of a given function and can be computed beforehand. The  $C_{j,k,l,m}^{\beta\alpha\pm}$  has the property

$$C_{j,k,-l,m}^{B\alpha-} = C_{-j,k,l,m}^{B\alpha+}, \quad (44)$$

because of the symmetry property of  $\tilde{\mathcal{L}}_J^{\beta\alpha}$  ( $J=1,2,3$ ) and the lattice of  $\zeta_1$  symmetric with respect to  $\zeta_1=0$ . Further,  $K^{\beta\alpha}$  and  $X_0^A$  are not contained in the integrals  $\tilde{\mathcal{L}}_1^{AA}(B_{l,m}^{\alpha+})$ ,  $\tilde{\mathcal{L}}_2^{BA}(B_{l,m}^{\alpha+})$ , etc. Thus we prepare the database of  $\tilde{\mathcal{L}}_1^{\beta\alpha}(B_{l,m}^{\beta+})_{(j,k)}$ ,  $\tilde{\mathcal{L}}_2^{\beta\alpha}(B_{l,m}^{\alpha+})_{(j,k)}$ , and  $\tilde{\mathcal{L}}_3^{\beta\alpha}(B_{l,m}^{\beta+})_{(j,k)}$  for different values of  $\hat{m}^B$  for  $j = -2N_1, \dots, 2N_1$ ,  $l = 0, \dots, 2N_1$ ,

and  $k, m = 0, \dots, 2N_\rho$ . The integration is performed accurately numerically by the Gauss–Legendre formula.<sup>54</sup> Then the numerical kernel  $C_{j,k,l,m}^{\beta\alpha\pm}$  is constructed from the database before the process of iteration by Eqs. (43a)–(43d). In the process of iteration, the computation of the collision integrals is a simple multiplication of matrices, i.e., Eqs. (42a) and (42b), and thus is performed efficiently.

## D. Chebyshev polynomials

One of the purposes of the present work is to provide the data for the slip boundary condition for the fluid-dynamic type system derived in Ref. 5 (see Sec. I). The slip condition is a linear combination of the thermal-slip and the diffusion-slip conditions given in Eq. (27). As is seen from Sec. III B, the slip coefficients  $b_I$  and  $b_{II}$  in Eq. (27) depend on the concentration  $X_0^A$ . But in the physical situations investigated in Ref. 5 the concentration generally varies along the boundary. Accordingly it is required to prepare formulas from which the values of  $b_I$  and  $b_{II}$  are readily obtained for arbitrary values of  $X_0^A$ . We use the Chebyshev polynomial approximation<sup>55</sup> with respect to  $X_0^A$  to meet this requirement. This approximation is useful not only for the slip coefficients but also for other physical quantities such as the Knudsen-layer functions. Therefore we describe it in general form.

Let us denote by  $T_n$  ( $n=0,1,2,\dots$ ) the Chebyshev polynomial defined for  $0 \leq \theta \leq \pi$  by the relation

$$T_n(\cos \theta) = \cos n\theta. \quad (45)$$

Any function  $F$  of  $X_0^A$  can be approximated by the polynomials of degree up to  $N$  in the Chebyshev basis as

$$F(X_0^A) = \sum_{n=0}^N a_n T_n(2X_0^A - 1), \quad (46)$$

where

$$a_n = \frac{1}{N\epsilon_n} \sum_{k=0}^{N-1} [F_k T_n(y_k) + F_{k+1} T_n(y_{k+1})], \quad (47)$$

with  $\epsilon_0 = \epsilon_N = 2$  and  $\epsilon_1 = \dots = \epsilon_{N-1} = 1$ , and

$$F_k = F\left(\frac{1+y_k}{2}\right), \quad (48)$$

with  $y_k$  being the Chebyshev abscissa:

$$y_k = \cos\left(k \frac{\pi}{N}\right) \quad (k=0,1,\dots,N). \quad (49)$$

The approximation (46) takes the exact value of  $F$  at  $X_0^A = (1+y_k)/2$ .

Since the function  $F$  of  $X_0^A$  is arbitrary, any physical quantity for an arbitrary value of  $X_0^A$  can be obtained by the formula (46) from its data computed at  $N+1$  discrete values of  $X_0^A$ , i.e.,  $X_0^A = (1+y_k)/2$  ( $k=0,1,\dots,N$ ).

## V. RESULTS AND DISCUSSIONS

In the present paper, we carry out the computation for  $m^B/m^A = 2, 4, 5$ , and 10 and for various values of  $X_0^A$ , restricting ourselves to the case  $d^B/d^A = 1$ . The computation for other values of  $d^B/d^A$  can be performed by using the

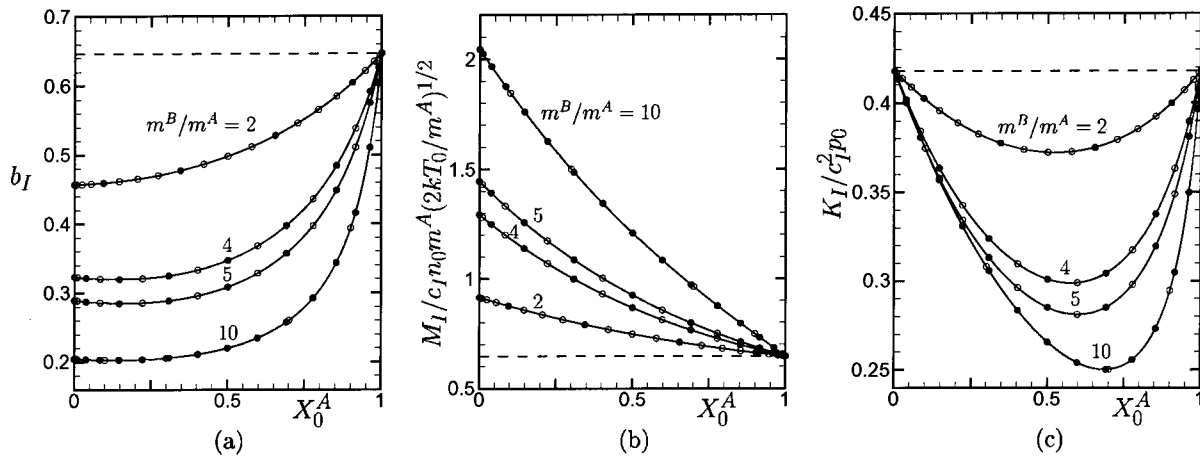


FIG. 1. Coefficient of thermal slip  $b_I$  and related quantities. (a) Slip coefficient  $b_I$ , (b) momentum  $M_I$  away from the wall, and (c) kinetic energy  $K_I$  per unit volume away from the wall. Both closed and open circles indicate the present result. The solid line indicates the present result using the formula (51). The data used to construct the formula are marked with a closed circle. The dashed line indicates the result for  $m^B/m^A = 1$ .

same code and database of  $\tilde{L}_1^{\beta\alpha}(B_{l,m}^{\beta+})_{(j,k)}$ ,  $\tilde{L}_2^{\beta\alpha}(B_{l,m}^{\alpha+})_{(j,k)}$ , etc. In what follows, we assume that  $m^B/m^A \geq 1$ , because the results for  $m^B/m^A < 1$  can be obtained from those for  $m^B/m^A > 1$  by a simple transformation.

**A. Slip coefficient**

The coefficient of thermal slip  $b_I$  vs the concentration  $X_0^A$  of gas A is shown in Fig. 1(a). Since  $b_I$  is positive, the flow induced along the wall is in the direction from the colder part to the hotter at a large distance from the wall. The  $b_I$  is larger for smaller molecular mass ratio  $m^B/m^A$  and becomes largest at  $m^B/m^A = 1$ . For  $m^B/m^A = 1$ , it is independent of  $X_0^A$  because there is no difference (except “color” or “label”) between molecules of a different kind. For  $m^B/m^A = 2$ ,  $b_I$  increases monotonically with increasing  $X_0^A$ , the concentration of the gas with smaller molecular mass. In contrast, for  $m^B/m^A = 4, 5$ , and  $10$ ,  $b_I$  first decreases slightly, takes the minimum at around  $X_0^A = 0.15 \sim 0.25$ , and then increases monotonically as  $X_0^A$  increases from zero to 1. At  $X_0^A = 1$ ,  $b_I$  is independent of  $m^B/m^A$  because of the absence of gas B. Incidentally, the values at  $X_0^A = 0$ , where gas A is

absent, are equal to the value at  $X_0^A = 1$  multiplied by  $(m^B/m^A)^{-1/2}$ . This relation is easily seen by changing the reference molecular mass from  $m^A$  to  $m^B$ .

The slip coefficient  $b_I$  corresponds to the flow velocity of the mixture away from the wall when  $c_I = 1$ . The momentum  $(0, M_I, 0)$  and the kinetic energy  $K_I$  per unit volume of the mixture away from the wall is related to  $b_I$  as follows:

$$M_I / c_I n_0 m^A (2kT_0/m^A)^{1/2} = \hat{\rho}_0 b_I, \tag{50}$$

$$K_I / c_I^2 p_0 = \hat{\rho}_0 b_I^2,$$

where  $\hat{\rho}_0 (\equiv \hat{m}^A X_0^A + \hat{m}^B X_0^B) = (1 - \hat{m}^B) X_0^A + \hat{m}^B$ . These quantities vs  $X_0^A$  are shown in Figs. 1(b) and 1(c). The momentum is larger for larger  $m^B/m^A$ . It decreases monotonically as  $X_0^A$  increases. The values at  $X_0^A = 0$  are the same as the value at  $X_0^A = 1$  multiplied by  $(m^B/m^A)^{1/2}$ . The kinetic energy is larger for smaller difference of mass. It takes the same value at  $X_0^A = 0$  and 1 and attains the minimum at an intermediate value of  $X_0^A$  ( $X_0^A = 0.5 \sim 0.7$ ).

The coefficient of diffusion slip  $b_{II}$  vs  $X_0^A$  is shown in Fig. 2(a). Since  $b_{II}$  is positive, the flow induced along

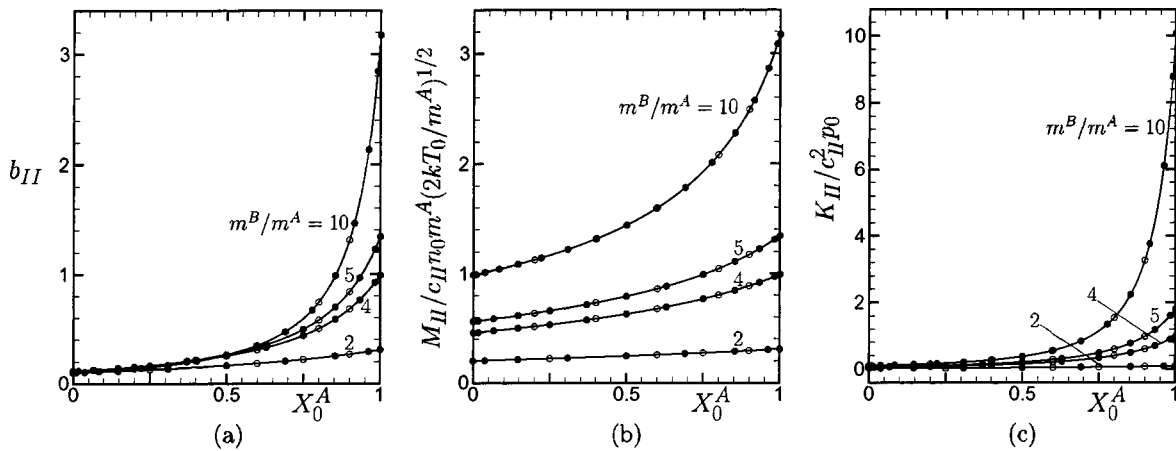


FIG. 2. Coefficient of diffusion slip  $b_{II}$  and related quantities. (a) Slip coefficient  $b_{II}$ , (b) momentum  $M_{II}$  away from the wall, and (c) kinetic energy  $K_{II}$  per unit volume away from the wall. See the caption of Fig. 1.

TABLE I. Coefficient  $b_I^{(n)}$  ( $n=0, \dots, N$ ) in Eq. (51) for the thermal-slip coefficient  $b_I$ .

$n$	$m^B/m^A$			
	2 ( $N=5$ )	4 ( $N=8$ )	5 ( $N=8$ )	10 ( $N=16$ )
0	7.636 42(-1) <sup>a</sup>	9.179 23(-1)	9.848 26(-1)	1.277 40
1	-1.326 32(-1)	-3.173 98(-1)	-3.923 97(-1)	-6.903 26(-1)
2	1.663 96(-2)	5.126 03(-2)	6.065 50(-2)	6.849 37(-2)
3	-1.251 75(-3)	-5.744 65(-3)	-7.004 42(-3)	-8.197 29(-3)
4	1.025 88(-4)	5.455 54(-4)	5.605 33(-4)	-3.541 47(-4)
5	-8.947 58(-6)	-1.012 07(-4)	-1.479 12(-4)	-3.841 75(-4)
6	-	8.148 85(-6)	4.051 81(-6)	-8.992 59(-5)
7	-	-1.853 88(-6)	-3.979 89(-6)	-3.471 91(-5)
8	-	1.637 69(-7)	-1.316 47(-7)	-1.145 87(-5)
9	-	-	-	-4.326 05(-6)
10	-	-	-	-1.592 96(-6)
11	-	-	-	-5.670 10(-7)
12	-	-	-	-1.869 57(-7)
13	-	-	-	-8.234 80(-8)
14	-	-	-	-4.147 64(-8)
15	-	-	-	-1.556 78(-8)
16	-	-	-	8.944 66(-10)

<sup>a</sup>Read as  $7.63642 \times 10^{-1}$ .

the wall in the far field is in the direction of increasing  $X_0^A + \tilde{C}_{II}^A X_2$ , i.e., from the part with lower concentration of the gas with smaller molecular mass to the part with higher concentration of the same gas. The  $b_{II}$  increases monotonically as  $X_0^A$  increases. It is larger for larger mass ratio  $m^B/m^A$  when  $X_0^A \geq 0.5$ . For smaller values of  $X_0^A$ , however, its dependence on  $m^B/m^A$  is not monotonic, and it becomes largest at around  $m^B/m^A = 4$  or 5. For  $m^B/m^A = 1$ , where there is no difference between molecules of different kind,  $b_{II}$  vanishes and thus the diffusion-slip flow is not induced. This fact can be shown analytically by making use of a property of  $D^{(\beta)\alpha}$  given in Appendix B of Ref. 56 and the existence and uniqueness theorem for the Knudsen-layer problem for a single-component gas (see Appendix C). In the meantime,  $b_{II}$  is nonzero at  $X_0^A = 0$  and 1. It appears strange at a glance because the ‘‘mixture’’ in these cases is, in reality, a single-component gas, where there is no diffusion-slip flow. However, at  $X_0^A = 0$  and 1, the concentration gradient  $\tilde{C}_{II}^A$  (or  $c_{II}$ ) should vanish because  $0 \leq X_0^A + \tilde{C}_{II}^A X_2 \leq 1$  by definition. Therefore, the diffusion-slip flow, which is the product of  $b_{II}$  and  $c_{II}$ , vanishes, and no contradiction arises.

The induced momentum ( $0, M_{II}, 0$ ) and the kinetic energy  $K_{II}$  per unit volume of the mixture away from the wall are shown in Figs. 2(b) and 2(c). They are related to the slip coefficient  $b_{II}$  through Eq. (50) with the subscript  $I$  being replaced by the subscript  $II$ . Both  $M_{II}$  and  $K_{II}$  are larger for larger  $m^B/m^A$  and for larger  $X_0^A$ .

As is seen from Figs. 1 and 2, the dependence of  $\hat{\rho}_0 b_J$  ( $J=I, II$ ) [cf. the first equation in Eq. (50) and the corresponding relation for  $M_{II}$ ] on  $X_0^A$  is simpler than that of  $b_J$ . Therefore we make the approximation formula of  $b_J$  for arbitrary values of  $X_0^A$  by applying Eq. (46) to  $\hat{\rho}_0 b_J$ , not directly to  $b_J$  itself. The data used to make the formula are shown with a closed circle in Figs. 1 and 2. The resulting formula is

TABLE II. Coefficient  $b_{II}^{(n)}$  ( $n=0, \dots, N$ ) in Eq. (51) for the diffusion-slip coefficient  $b_{II}$ .

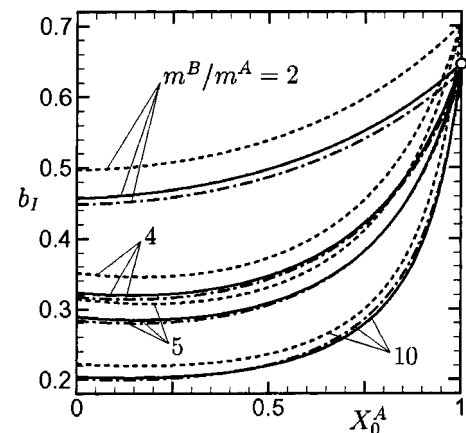
$n$	$m^B/m^A$			
	2 ( $N=8$ )	4 ( $N=12$ )	5 ( $N=12$ )	10 ( $N=16$ )
0	2.497 93(-1) <sup>a</sup>	6.732 35(-1)	8.662 87(-1)	1.719 82
1	5.316 06(-2)	2.551 79(-1)	3.687 19(-1)	9.666 00(-1)
2	4.271 74(-3)	4.686 53(-2)	8.075 02(-2)	3.142 93(-1)
3	5.144 04(-4)	1.015 04(-2)	2.001 50(-2)	1.095 60(-1)
4	4.721 89(-5)	2.123 51(-3)	4.947 61(-3)	3.944 40(-2)
5	5.628 93(-6)	4.696 41(-4)	1.267 93(-3)	1.451 52(-2)
6	5.546 15(-7)	1.031 65(-4)	3.270 88(-4)	5.423 39(-3)
7	6.634 70(-8)	2.318 88(-5)	8.562 21(-5)	2.048 47(-3)
8	6.740 49(-9)	5.217 45(-6)	2.255 15(-5)	7.802 44(-4)
9	-	1.188 34(-6)	5.986 59(-6)	2.990 82(-4)
10	-	2.705 43(-7)	1.603 65(-6)	1.152 47(-4)
11	-	6.449 01(-8)	4.584 02(-7)	4.460 01(-5)
12	-	1.427 69(-8)	1.149 78(-7)	1.734 05(-5)
13	-	-	-	6.776 19(-6)
14	-	-	-	2.702 63(-6)
15	-	-	-	1.191 30(-6)
16	-	-	-	4.125 02(-7)

<sup>a</sup>Read as  $2.49793 \times 10^{-1}$ .

$$b_J = \sum_{n=0}^N b_J^{(n)} T_n(2X_0^A - 1) / \hat{\rho}_0 \quad (J=I, II), \quad (51)$$

with  $\hat{\rho}_0 = (1 - \hat{m}^B) X_0^A + \hat{m}^B$  and the data of  $b_I^{(n)}$  and  $b_{II}^{(n)}$  listed in Tables I and II. The solid lines in Figs. 1 and 2 are drawn by using this formula.

The thermal-slip and the diffusion-slip problems for a mixture have been studied by various approximation methods (the variational method, the moment method, etc.) or by the direct computation of model Boltzmann equations. Some of the approximation methods aim at providing the slip coefficients for different molecular models, including the more realistic Lennard-Jones potential. In contrast, in the present paper, we have analyzed the Boltzmann equation faithfully and accurately, restricting ourselves to the hard-sphere molecules. Our aim is to establish reliable results at the level of the velocity distribution functions that can serve as the standard solutions for these two problems for the hard-sphere

FIG. 3. A comparison with the previous results:  $b_I$  vs  $X_0^A$ . The solid line indicates the present result, the dashed line the formula in Ref. 34, the dot-dashed line that in Ref. 38, and the open circle the result in Ref. 12.

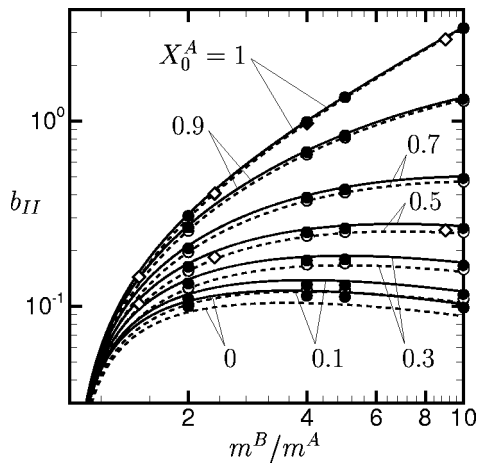


FIG. 4. A comparison with the previous results II:  $b_{II}$  vs  $m^B/m^A$  for  $X_0^A = 0, 0.1, 0.3, 0.5, 0.7, 0.9,$  and  $1$ . The closed circle indicates the present result; the dashed line the formula in Ref. 34; the solid line that in Ref. 38; the open circle the result in Ref. 39 for  $X_0^A = 0.1, 0.3, 0.5, 0.7,$  and  $0.9$ ; and the open diamond that in Ref. 33 for  $X_0^A = 0.5$  and  $0.99$ .

molecular model that is not necessarily realistic but is the most fundamental model in kinetic theory. Such standard solutions are useful to validate convenient expressions for the slip coefficients obtained by approximation methods that can be extended to more realistic models rather easily. By the way, it should be mentioned that the extension of the present method to other molecular models is straightforward though it gives rise to some complexity.

Keeping the above discussion in mind, we now compare the present result with existing results obtained by other approximation methods. When the latter contain the results for other molecular models, we take only those for the hard-sphere molecules in the comparison. Figures 3 and 4 and

Tables III and IV show such a comparison. It is seen that among the existing results the formula in Ref. 38, which is derived by a special kind of half-space moment method with the second-order Chapman–Enskog expansions, agrees best to the present result. In the figures and the tables, the formula in Ref. 34, which is derived by the same method as Ref. 38 with the first-order Chapman–Enskog expansions, is also shown. Incidentally, this formula is the same in its form as the formula in Ref. 29 that is derived by the use of variational principle and the first-order Chapman–Enskog expansions. The formula given in Ref. 32, where the simplification of the approximate formulas<sup>29,34</sup> is discussed, shows less agreement with the present result. The results by Yalamov, Yushkanov, and Savkov<sup>33</sup> (half-space moment method) and by Sharipov and Kalempa<sup>39</sup> (finite-difference analysis based on the McCormack model<sup>57</sup>) are close to the formula in Ref. 34 rather than to the present result.

The open circle at  $X^A = 1$  in Fig. 3 indicates the thermal-slip coefficient for a single-component hard-sphere gas obtained by the finite-difference method on which the present method is based.<sup>12</sup> It should be mentioned that Loyalka<sup>31</sup> has obtained essentially the same value. He numerically solved an approximate linearized Boltzmann equation that is derived by taking the first five terms of the expansion of the collision-integral kernel in terms of the associate Legendre functions.<sup>31,58</sup> According to Ref. 23, the deviation of the approximate kernel from the original one is not small (in fact, the singularity contained in the original kernel is not reproduced by the approximate kernel). In this sense, the equation is not necessarily a good approximation of the linearized Boltzmann equation. Nevertheless, the thermal-slip coefficient obtained from this equation is accurate. Recently, Siewert developed an efficient and accurate method for a single-component gas by combining the approximate equation

TABLE III. A comparison with the previous results for the thermal-slip coefficient  $b_I$ .

$m^B/m^A$	$X_0^A = 0.1$				
	Present result	Ref. 32	Ref. 33	Ref. 34	Ref. 38
2	0.4599	0.5023	–	0.4993	0.4507
4	0.3199	0.3515	–	0.3466	0.3141
5	0.2854	0.3140	–	0.3091	0.2804
10	0.2028	0.2242	–	0.2200	0.1997
$m^B/m^A$	$X_0^A = 0.5$				
	Present result	Ref. 32	Ref. 33	Ref. 34	Ref. 38
1.5	–	0.6193	0.631	0.6142	0.5521
2	0.4981	0.5514	–	0.5389	0.4869
7/3	–	0.5149	0.513	0.4984	0.4518
4	0.3469	0.4000	0.385	0.3726	0.3424
5	0.3082	0.3604	–	0.3308	0.3056
9	–	0.2776	0.259	0.2475	0.2313
10	0.2198	0.2655	–	0.2360	0.2209
$m^B/m^A$	$X_0^A = 0.9$				
	Present result	Ref. 32	Ref. 33	Ref. 34	Ref. 38
2	0.6023	0.6616	–	0.6539	0.5911
4	0.5231	0.5975	–	0.5668	0.5183
5	0.4929	0.5743	–	0.5341	0.4912
10	0.3937	0.4951	–	0.4273	0.4030

TABLE IV. A comparison with the previous results for the diffusion-slip coefficient  $b_{II}$ .

		$X_0^A=0.1$				
$m^B/m^A$	Present result	Ref. 32	Ref. 33	Ref. 34	Ref. 38	Ref. 39
2	0.1098	0.0470	–	0.1022	0.1163	0.1030
4	0.1309	0.0644	–	0.1202	0.1384	0.1234
5	0.1300	0.0661	–	0.1189	0.1369	0.1227
10	0.1155	0.0624	–	0.1046	0.1201	0.1093
		$X_0^A=0.5$				
$m^B/m^A$	Present result	Ref. 32	Ref. 33	Ref. 34	Ref. 38	Ref. 39
1.5	–	0.0451	0.103	0.0990	0.1088	–
2	0.1637	0.0769	–	0.1549	0.1702	0.1550
7/3	–	0.0930	0.184	0.1797	0.1974	–
4	0.2514	0.1378	0.243	0.2373	0.2605	0.2399
5	0.2634	0.1493	–	0.2486	0.2728	0.2517
9	–	0.1597	0.257	0.2503	0.2742	–
10	0.2619	0.1590	–	0.2473	0.2709	0.2513
		$X_0^A=0.9$				
$m^B/m^A$	Present result	Ref. 32	Ref. 33	Ref. 34	Ref. 38	Ref. 39
2	0.2666	0.1340	–	0.2569	0.2728	0.2552
4	0.6805	0.4012	–	0.6646	0.6923	0.6598
5	0.8365	0.5094	–	0.8200	0.8513	0.8133
10	1.311	0.8575	–	1.2998	1.3412	1.2816

based on more terms (nine terms) of the kernel expansion and his analytical discrete-ordinate method.<sup>40</sup> This gives an accurate result for the velocity and heat-flow profiles as well as the slip coefficient for a single-component gas by fast computation. It should be stressed, however, that the result obtained by the direct numerical analysis in Refs. 12 and 23 served to assess the new method. Incidentally, the Siewert method has been used for a more sophisticated model of the

boundary condition (the so-called Cercignani–Lampis model<sup>59</sup>).

## B. Knudsen-layer functions

The Knudsen-layer functions of component gases  $U^A$  and  $U^B$  for the thermal slip (problem I) are shown in Fig. 5 and in Tables V and VI, and  $H^A/X_0^A$  and  $H^B/X_0^B$  are in the

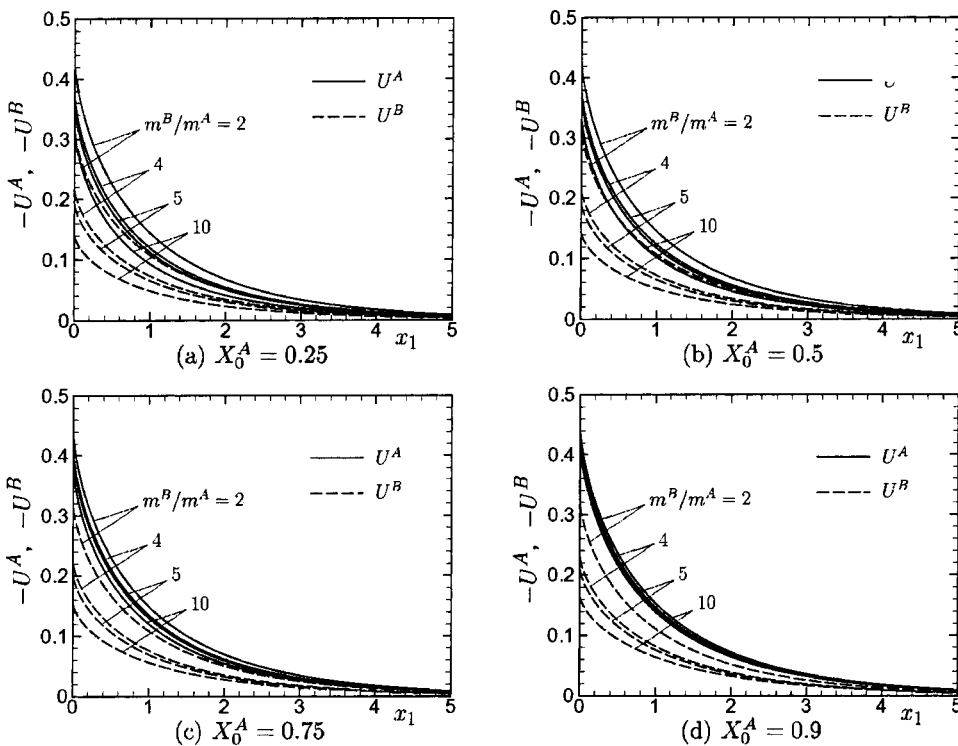


FIG. 5. Knudsen-layer functions  $U^A$  and  $U^B$  for the thermal slip (problem I). (a)  $X_0^A=0.25$ , (b)  $X_0^A=0.5$ , (c)  $X_0^A=0.75$ , and (d)  $X_0^A=0.9$ .



TABLE VII. Knudsen-layer function  $-S^A/X_0^A$  for the thermal slip (problem I) in the case  $m^B/m^A=2$  and 5.

$x_1 \backslash X_0^A$	$m^B/m^A=2$			$m^B/m^A=5$		
	0.25	0.5	0.75	0.25	0.5	0.75
0.0000	0.0281	0.0188	0.0096	0.0420	0.0288	0.0152
0.0283	0.0281	0.0188	0.0095	0.0418	0.0287	0.0151
0.0516	0.0280	0.0187	0.0095	0.0416	0.0286	0.0151
0.0973	0.0278	0.0186	0.0094	0.0412	0.0282	0.0149
0.1435	0.0275	0.0184	0.0094	0.0406	0.0278	0.0146
0.2005	0.0271	0.0181	0.0092	0.0399	0.0273	0.0143
0.2934	0.0263	0.0176	0.0090	0.0385	0.0264	0.0138
0.4052	0.0253	0.0169	0.0086	0.0367	0.0251	0.0132
0.5010	0.0243	0.0163	0.0083	0.0352	0.0241	0.0126
0.5703	0.0237	0.0159	0.0081	0.0340	0.0233	0.0122
0.7611	0.0217	0.0146	0.0075	0.0310	0.0212	0.0111
0.9749	0.0197	0.0133	0.0068	0.0277	0.0191	0.0100
1.1604	0.0180	0.0121	0.0062	0.0251	0.0173	0.0091
1.3574	0.0163	0.0110	0.0057	0.0225	0.0156	0.0083
1.6176	0.0142	0.0096	0.0050	0.0195	0.0136	0.0072
1.9474	0.0119	0.0081	0.0042	0.0162	0.0113	0.0061
2.4121	0.0093	0.0064	0.0033	0.0124	0.0088	0.0048
2.9000	0.0071	0.0049	0.0026	0.0093	0.0067	0.0037
3.3427	0.0055	0.0038	0.0020	0.0072	0.0052	0.0030
3.8645	0.0041	0.0029	0.0015	0.0053	0.0039	0.0023
4.8136	0.0024	0.0017	0.0009	0.0030	0.0023	0.0014
5.7335	0.0014	0.0010	0.0006	0.0018	0.0014	0.0009
7.6095	0.0005	0.0003	0.0002	0.0006	0.0005	0.0003
9.5607	0.0002	0.0001	0.0001	0.0002	0.0002	0.0001
11.4142	0.0001	0.0000	0.0000	0.0001	0.0001	0.0000
15.2205	0.0000	0.0000	0.0000	0.0000	0.0000	0.0000

same tables. Each function decays monotonically and rapidly to zero as the distance from the wall increases. These functions depend monotonically on the mass ratio  $m^B/m^A$ . For  $U^A$  and  $H^A/X_0^A$ , the dependence is larger for smaller  $X_0^A$ , the

TABLE VIII. Knudsen-layer functions  $U^A$  and  $H^A$  for the thermal slip (problem I) in the case  $X_0^A=1$ .

$x_1$	$-U^A$	$H^A$
0.0000	0.4452	1.3895
0.0283	0.4161	1.2794
0.0516	0.3995	1.2178
0.0973	0.3730	1.1215
0.1435	0.3509	1.0426
0.2005	0.3275	0.9609
0.2934	0.2956	0.8519
0.4052	0.2639	0.7467
0.5010	0.2409	0.6722
0.5703	0.2260	0.6251
0.7611	0.1913	0.5173
0.9749	0.1602	0.4243
1.1604	0.1383	0.3604
1.3574	0.1189	0.3052
1.6176	0.0979	0.2470
1.9474	0.0771	0.1909
2.4121	0.0556	0.1348
2.9000	0.0399	0.0949
3.3427	0.0297	0.0697
3.8645	0.0211	0.0488
4.8136	0.0115	0.0261
5.7335	0.0064	0.0145
7.6095	0.0020	0.0045
9.5607	0.0006	0.0014
11.4142	0.0002	0.0005
15.2205	0.0000	0.0000

concentration of the gas with smaller molecular mass, while for  $U^B$  and  $H^B/X_0^B$ , it is little influenced by the value of  $X_0^A$ . On the other hand, the dependence on  $X_0^A$  differs among the functions. The functions  $U^A$  and  $H^A/X_0^A$  depend on  $X_0^A$  especially when  $m^B/m^A$  is large. This is also true for  $U^B$ , but less dependent on  $X_0^A$ . The  $H^B/X_0^B$  is almost independent of  $X_0^A$  irrespective of  $m^B/m^A$ .

The function  $S^A/X_0^A$  is shown in Table VII. The results for  $m^B/m^A=4$  and 10 are omitted, but they are very close to that for  $m^B/m^A=5$ . It is seen that  $S^A/X_0^A$  decays monotonically and rapidly to zero as  $x_1 \rightarrow \infty$  and that it depends on  $X_0^A$  monotonically. The function  $S^B$  can be obtained from the table by the relation (26).

The functions  $U^A$  and  $H^A$  for  $X_0^A=1$  are shown in Table VIII. Since gas B is absent in this case, they are independent of  $m^B/m^A$  and can be regarded as the counterparts of a single-component gas. From a different viewpoint, they can also be regarded as  $U^A$  and  $H^A/X_0^A$  for arbitrary values of  $X_0^A$  in the case of  $m^B/m^A=1$ . It is also seen from a change of a role between gas A and B that  $U^B$  and  $H^B/X_0^B$  at  $X_0^A=0$  are, respectively,  $U^A$  and  $H^A$  in the table multiplied by  $(m^B/m^A)^{-1/2}$ . Incidentally, the corresponding Knudsen-layer functions for a single-component gas have already been obtained in Ref. 12 by the same numerical method, i.e., the finite-difference method incorporating the numerical kernel method. In the present work, they are obtained with higher accuracy, but the difference is at most  $1.1 \times 10^{-4}$  for  $U^A$  and  $1.8 \times 10^{-4}$  for  $H^A$ .

The Knudsen-layer functions  $U^A$  and  $U^B$  for the diffusion slip (problem II) are shown in Fig. 6 and in Tables IX





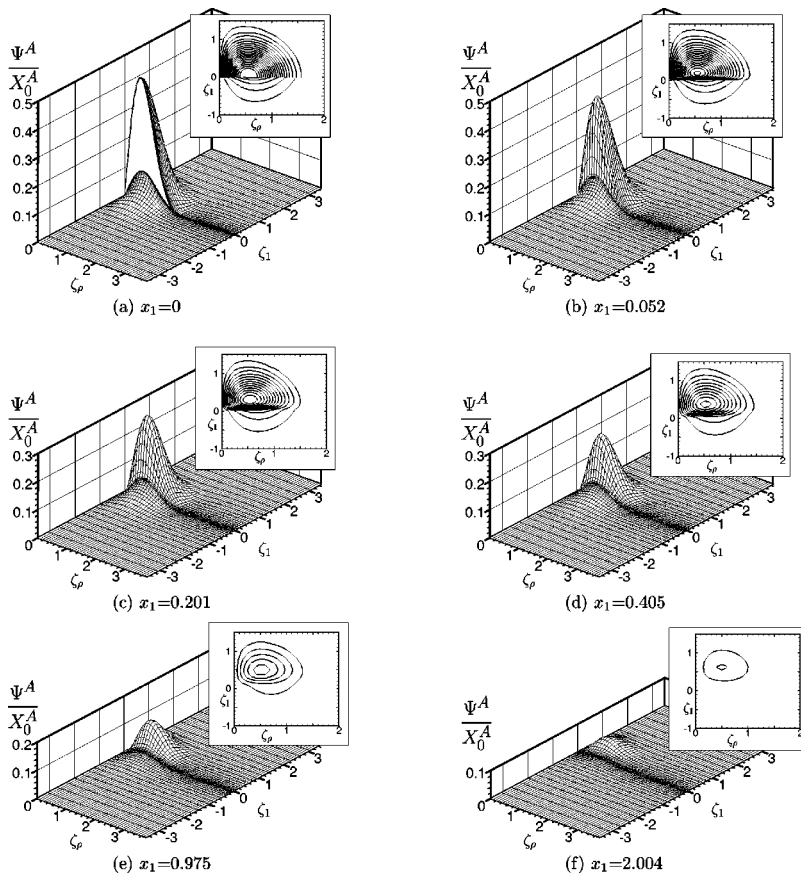


FIG. 7. Reduced velocity distribution function  $\Psi^A/X_0^A$  of gas A and its contour plots for the thermal slip (problem I) in the case of  $m^B/m^A=5$  and  $X_0^A=0.5$ . (a)  $x_1=0$ , (b)  $x_1=0.052$ , (c)  $x_1=0.201$ , (d)  $x_1=0.405$ , (e)  $x_1=0.975$ , and (f)  $x_1=2.004$ . In the contour plots the curves are drawn with the interval 0.02. The outermost curve indicates the contour  $\Psi^A/X_0^A=0.02$ .

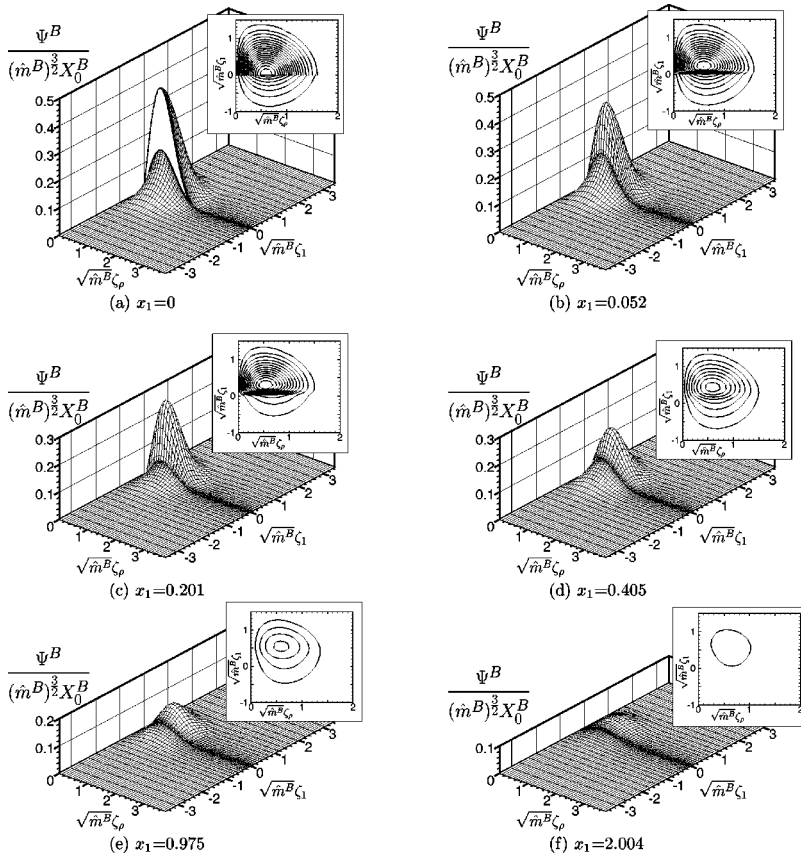


FIG. 8. Reduced velocity distribution function  $\Psi^B/((m^B)^{3/2}X_0^B)$  of gas B and its contour plots for the thermal slip (problem I) in the case of  $m^B/m^A=5$  and  $X_0^A=0.5$ . (a)  $x_1=0$ , (b)  $x_1=0.052$ , (c)  $x_1=0.201$ , (d)  $x_1=0.405$ , (e)  $x_1=0.975$ , and (f)  $x_1=2.004$ . See the caption of Fig. 7.

TABLE XII. Lattice systems.

Lattice system	$d$	$\bar{N}_x$	$N_x$	$\bar{Z}_1$	$\bar{Z}_\rho$	$Z_1$	$Z_\rho$	$\bar{N}_1$	$\bar{N}_\rho$	$N_1$	$N_\rho$
S1	24.08	300	300	–	–	–	–	–	–	–	–
S2	24.08	600	600	–	–	–	–	–	–	–	–
S3	27.74	300	320	–	–	–	–	–	–	–	–
S4	32.20	300	340	–	–	–	–	–	–	–	–
M1	–	–	–	4.5	4.5	4.5	4.5	25	27	25	27
M2	–	–	–	4.5	4.5	4.5	4.5	25	36	25	36
M3	–	–	–	4.5	4.5	4.5	4.5	25	24	25	24
M4	–	–	–	4.5	4.5	4.5	4.5	28	24	28	24
M5	–	–	–	4.5	4.5	4.5	4.5	28	18	28	18
M6	–	–	–	4.5	4.5	5.0	5.25	28	18	29	21
M7	–	–	–	4	4	4	4	18	10	18	10
M8	–	–	–	4.5	4.5	4.5	4.5	25	18	25	18

larger for larger difference of molecular mass. The  $S^B$  can be obtained again from the table by the relation (26).

Incidentally, some of the results for  $X_0^A = 0.25, 0.75,$  and  $0.9$  in the figures and tables in this section are obtained by applying the formula (46) to the functions  $U^A, U^B, H^A/X_0^A, H^B/X_0^B,$  and  $S^A/X_0^A$  for problem I and to  $X_0^A U^A, X_0^B U^B, H^A, H^B,$  and  $S^A$  for problem II. The FORTRAN code generating the Knudsen-layer functions for an arbitrary value of  $X_0^A$  is available from the authors.

### C. Velocity distribution functions

Figures 7 and 8 show the reduced velocity distribution functions  $\Psi^A$  and  $\Psi^B$  and their contour plots for the thermal-slip problem (problem I) in the case of  $m^B/m^A = 5$  and  $X_0^A = 0.5$ . There is a discontinuity at  $\zeta_1 = 0$  on the wall ( $x_1 = 0$ ) [see Figs. 7(a) and 8(a)]. The discontinuity disappears inside the gas. This is because the characteristic line of the Boltzmann equation (18) along  $\zeta_1 = 0$  does not enter the gas region, so that the discontinuity does not propagate into the gas.<sup>53</sup> Its trace remains, however, as a steep gradient around  $\zeta_1 = 0$  near the wall [see Figs. 7(b) and 8(b)]. As the distance from the wall increases,  $\Psi^\alpha$  is deformed chiefly around  $\zeta_1 = 0$  with keeping the difference of shape between the positive and the negative regions of  $\zeta_1$  and decays to zero [see the transition from Fig. 7(a) to 7(f) and from Fig. 8(a) to 8(f)]. These are true also for other cases.

A comparison with the other cases shows that the function  $\Psi^B/((\hat{m}^B)^{3/2}X_0^B)$  is almost independent of  $\hat{m}^B$  and  $X_0^A$  if it is considered as a function of  $\sqrt{\hat{m}^B}\zeta_1$  and  $\sqrt{\hat{m}^B}\zeta_\rho$ . On the other hand, the function  $\Psi^A/X_0^A$  rather depends on  $\hat{m}^B$

and  $X_0^A$  mainly in  $\zeta_1 < 0$  region. The difference between  $\zeta_1 > 0$  and  $\zeta_1 < 0$  regions is larger for larger  $\hat{m}^B$  and for smaller  $X_0^A$ .

We omit the results for the diffusion-slip problem because an example of the reduced velocity distribution function has already been shown in Ref. 25. The qualitative features are the same as those described in the first paragraph.

### VI. DATA OF COMPUTATION

In the present work, we use the following lattice systems:

$$x_1^{(i)} = 20 \ln(p^{(\bar{N}_x)} / (p^{(\bar{N}_x)} - 0.7p^{(i)})) + 10^{-4} \left( \frac{i}{\bar{N}_x} \right) \quad (i = 0, 1, \dots, N_x), \quad (52a)$$

with

$$p^{(i)} = 25(i^3/\bar{N}_x^2) / [1 + 25(i/\bar{N}_x)^2], \quad (52b)$$

and

$$\zeta_1^{\alpha(2j)} = (\bar{Z}_1/\sqrt{\hat{m}^\alpha})(j/\bar{N}_1)^3 \quad (j = -N_1, \dots, N_1), \quad (53a)$$

$$\zeta_1^{\alpha(2j+1)} = (\zeta_1^{\alpha(2j)} + \zeta_1^{\alpha(2j+2)})/2 \quad (j = -N_1, \dots, N_1 - 1), \quad (53b)$$

$$\zeta_\rho^{\alpha(k)} = (\bar{Z}_\rho/\sqrt{\hat{m}^\alpha})(k/2\bar{N}_\rho) \quad (k = 0, \dots, 2N_\rho). \quad (53c)$$

TABLE XIII. A comparison of  $b_I$  among the different lattice systems for  $m^B/m^A = 2$ .

Lattice systems	Maximum relative error of $b_I$
(S1,M7) vs (S3,M7) <sup>a</sup>	$7.8 \times 10^{-7}$
(S1,M5) vs (S1,M6)	$3.7 \times 10^{-6}$
(S1,M7) vs (S2,M7)	$6.6 \times 10^{-6}$
(S1,M3) vs (S1,M4)	$2.3 \times 10^{-6}$
(S1,M3) vs (S1,M1)	$2.1 \times 10^{-5}$
(S1,M1) vs (S1,M2) <sup>a</sup>	$3.5 \times 10^{-5}$

<sup>a</sup>This case was checked only for  $X_0^A = 1$ , while the others were for 8 sample values of  $X_0^A$ .

TABLE XIV. A comparison of  $b_{II}$  among the different lattice systems for  $m^B/m^A = 2$ .

Lattice systems	Maximum relative error of $b_{II}$
(S1,M7) vs (S3,M7) <sup>a</sup>	$1.7 \times 10^{-7}$
(S1,M7) vs (S2,M7) <sup>a</sup>	$1.9 \times 10^{-7}$
(S1,M5) vs (S1,M6) <sup>a</sup>	$5.6 \times 10^{-7}$
(S1,M8) vs (S1,M5) <sup>b</sup>	$9.1 \times 10^{-6}$
(S1,M8) vs (S1,M3) <sup>b</sup>	$8.0 \times 10^{-5}$
(S1,M3) vs (S1,M1) <sup>c</sup>	$1.9 \times 10^{-5}$

<sup>a</sup>This case was checked only for  $X_0^A = 0.5$ .

<sup>b</sup>This case was checked for 9 sample values of  $X_0^A$ .

<sup>c</sup>This case was checked for 5 sample values of  $X_0^A$ .

TABLE XV. Maximum error of the integrals  $\tilde{\mathcal{L}}^{\beta\alpha}(f^\beta, f^\alpha)$  with  $f^\alpha = \hat{m}^\alpha \zeta_\rho E^\alpha$ . The data for system M1 are shown in the upper line and those for system M3 in the lower. The maximum value of  $|\nu^\beta f^\alpha E^\alpha|$  is also shown for comparison in parentheses.

$(\beta, \alpha)$	$m^B/m^A$			
	2	4	5	10
(A,A)	$3.51 \times 10^{-6}$ $4.46 \times 10^{-6}$ (0.064)			
(B,A)	$1.89 \times 10^{-6}$ $2.46 \times 10^{-6}$ (0.053)	$2.64 \times 10^{-6}$ $3.29 \times 10^{-6}$ (0.047)	$3.03 \times 10^{-6}$ $3.77 \times 10^{-6}$ (0.046)	$5.06 \times 10^{-6}$ $6.42 \times 10^{-6}$ (0.043)
(A,B)	$6.15 \times 10^{-6}$ $7.92 \times 10^{-6}$ (0.237)	$3.24 \times 10^{-5}$ $4.14 \times 10^{-5}$ (0.908)	$5.94 \times 10^{-5}$ $7.61 \times 10^{-5}$ (1.407)	$4.11 \times 10^{-4}$ $5.32 \times 10^{-4}$ (5.528)
(B,B)	$9.93 \times 10^{-6}$ $1.26 \times 10^{-5}$ (0.182)	$2.81 \times 10^{-5}$ $3.57 \times 10^{-5}$ (0.514)	$3.93 \times 10^{-5}$ $4.99 \times 10^{-5}$ (0.719)	$1.11 \times 10^{-4}$ $1.41 \times 10^{-4}$ (2.033)

Here  $\bar{N}_x$ ,  $\bar{N}_1$ , and  $\bar{N}_\rho$  are given positive integers and  $\bar{Z}_1$  and  $\bar{Z}_\rho$  are given constants.

The lattice systems generated by Eqs. (52a)–(53c) and used for various accuracy tests are listed in Table XII. Comparisons among the results for different lattice systems were made for various purposes in the case of  $m^B/m^A=2$ . A part of the results are shown in Tables XIII and XIV. For example, for problem I, a comparison is made between the systems (S1,M7) and (S3,M7) for an estimate of the appropriate value of  $d$ . Similarly a comparison is made between (S1,M5) and (S1,M6) for an estimate of the appropriate values of  $Z_1$  and  $Z_\rho$ . The comparison between (S1,M7) and (S2,M7) is for determining the number of lattice points  $N_x$  in  $x_1$ . The comparisons among (S1,M1), (S1,M2), (S1,M3), and (S1,M4) are for determining the number of points  $(N_1, N_\rho)$  in  $(\zeta_1, \zeta_\rho)$ . After such a series of tests, the system (S1,M1) is chosen as the standard lattice system for problem I, (S1,M3) for problem II in the case  $m^B/m^A=2$ , and (S4, M3) for problem II in the case  $m^B/m^A=4, 5, 10$ . The data in Sec. V are the results for these systems.

In order to estimate the accuracy of the collision integrals for the standard lattice systems, we make use of three properties of  $\tilde{\mathcal{L}}^{\beta\alpha}$ . The first is that the relation  $\tilde{\mathcal{L}}^{\beta\alpha}(\hat{m}^\beta \zeta_\rho E^\beta, \hat{m}^\alpha \zeta_\rho E^\alpha) = 0$  should hold. This comes from the fact that the original linearized collision integrals vanish when the collision invariants are substituted. Table XV shows the maximum error of the quantity on the left for the

TABLE XVI. Maximum error of the left-hand side of Eq. (54) for 6 sample values of  $X_0^A$  for system M1. The maximum value of  $|\zeta_\rho(\hat{m}^\alpha \zeta^2 - \frac{5}{2})E^\alpha|$  is also shown for comparison in parentheses just below the data.

$\alpha$	$m^B/m^A$			
	2	4	5	10
A	$1.58 \times 10^{-5}$ (0.16)	$1.58 \times 10^{-5}$ (0.16)	$1.58 \times 10^{-5}$ (0.16)	$2.01 \times 10^{-5}$ (0.16)
B	$3.12 \times 10^{-5}$ (0.32)	$6.30 \times 10^{-5}$ (0.64)	$7.88 \times 10^{-5}$ (0.81)	$3.71 \times 10^{-4}$ (1.61)

TABLE XVII. Maximum error of the left-hand side of Eq. (55) for 6 sample values of  $X_0^A$  for system M3. The maximum value of  $|\zeta_\rho(\delta_{\alpha A} - \delta_{\alpha B})E^\alpha|$  is also shown for comparison in parentheses just below the data.

$\alpha$	$m^B/m^A$			
	2	4	5	10
A	$1.39 \times 10^{-5}$ (0.077)	$2.43 \times 10^{-5}$ (0.077)	$2.91 \times 10^{-5}$ (0.077)	$5.26 \times 10^{-5}$ (0.077)
B	$1.19 \times 10^{-5}$ (0.15)	$5.48 \times 10^{-5}$ (0.31)	$9.66 \times 10^{-5}$ (0.38)	$6.12 \times 10^{-4}$ (0.77)

systems M1 and M3. The error comes from the part  $\tilde{\mathcal{L}}_1^{\beta\alpha} + \tilde{\mathcal{L}}_2^{\beta\alpha} - \tilde{\mathcal{L}}_3^{\beta\alpha}$  because  $\nu^\beta$  can be computed exactly [note that the integral in Eq. (23) is the error function]. The maximum value of  $|\hat{m}^\alpha \zeta_\rho E^\alpha \nu^\beta|$  is, therefore, shown in parentheses in the table. The second is that the relation,

$$\sum_{\beta=A,B} K^{\beta\alpha} X_0^\beta \tilde{\mathcal{L}}^{\beta\alpha}(\zeta_\rho A^\beta E^\beta, \zeta_\rho A^\alpha E^\alpha) + \zeta_\rho \left( \hat{m}^\alpha \zeta^2 - \frac{5}{2} \right) E^\alpha = 0, \quad (54)$$

which comes from Eq. (9a), should hold. The maximum error of the quantity on the left for the system M1 is shown in Table XVI, together with the maximum value of  $|\zeta_\rho(\hat{m}^\alpha \zeta^2 - 5/2)E^\alpha|$  in parentheses. The last is the relation

$$\sum_{\beta=A,B} K^{\beta\alpha} X_0^\alpha X_0^\beta \tilde{\mathcal{L}}^{\beta\alpha}(\zeta_\rho D^{(AB)\beta} E^\beta, \zeta_\rho D^{(AB)\alpha} E^\alpha) + \zeta_\rho E^\alpha (\delta_{\alpha A} - \delta_{\alpha B}) = 0, \quad (55)$$

with  $D^{(AB)\alpha} = D^{(A)\alpha} - D^{(B)\alpha}$ . The relation comes from Eq. (9b). The maximum error of the quantity on the left for the system M3 is shown in Table XVII, together with the maximum value of  $|\zeta_\rho E^\alpha (\delta_{\alpha A} - \delta_{\alpha B})|$  in parentheses.

As mentioned in Sec. III C, Eq. (26) provides another measure of accuracy. For the standard lattice system the value of  $|S^A + S^B|$ , which should theoretically be zero, is bounded as follows: for problem I,

$$|S^A + S^B| < \begin{cases} 2.57 \times 10^{-5} & (m^B/m^A = 2, 4, 5), \\ 3.28 \times 10^{-5} & (m^B/m^A = 10), \end{cases}$$

at 21 ( $m^B/m^A=2$ ) or 17 (the other cases,  $\zeta$ ) sample values of  $X_0^A$ , and for problem II,

$$|S^A + S^B| < \begin{cases} 2.74 \times 10^{-5} & (m^B/m^A = 2, 4, 5), \\ 2.93 \times 10^{-4} & (m^B/m^A = 10), \end{cases}$$

at 9 ( $m^B/m^A=2$ ), 13 ( $m^B/m^A=4,5$ ), or 17 ( $m^B/m^A=10$ ) sample values of  $X_0^A$ . For the same values of  $X_0^A$ , we compared the maximum values of  $|\Psi^\alpha(d, \cdot, \cdot)|$ ,  $|\Psi^\alpha(\cdot, \pm Z_1, \cdot)|$ , and  $|\Psi^\alpha(\cdot, \cdot, Z_\rho^\alpha)|$  to the maximum value of  $|\Psi^\alpha|$ . The former three values should be negligible in order that the computation in the finite region of  $(x_1, \zeta_1, \zeta_\rho)$  is justified. The results are

$$\frac{|\Psi^A(d, \cdot, \cdot)|}{\max|\Psi^A|} < \begin{cases} 8.3 \times 10^{-8} & (m^B/m^A = 2, 4, 5), \\ 2.9 \times 10^{-7} & (m^B/m^A = 10), \end{cases}$$

$$\frac{|\Psi^B(d, \cdot, \cdot)|}{\max|\Psi^B|} < \begin{cases} 2.6 \times 10^{-7} & (m^B/m^A = 2, 4, 5), \\ 3.0 \times 10^{-6} & (m^B/m^A = 10), \end{cases}$$

$$\frac{\max(|\Psi^A(\cdot, \pm Z_1^A, \cdot)|, |\Psi^A(\cdot, \cdot, Z_\rho^A)|)}{\max|\Psi^A|} < 5.7 \times 10^{-8},$$

$$\frac{\max(|\Psi^B(\cdot, \pm Z_1^B, \cdot)|, |\Psi^B(\cdot, \cdot, Z_\rho^B)|)}{\max|\Psi^B|} < 8.6 \times 10^{-8},$$

for problem I and

$$\frac{|\Psi^A(d, \cdot, \cdot)|}{\max|\Psi^A|} < \begin{cases} 4.9 \times 10^{-8} & (m^B/m^A = 2, 4, 5), \\ 2.5 \times 10^{-6} & (m^B/m^A = 10), \end{cases}$$

$$\frac{|\Psi^B(d, \cdot, \cdot)|}{\max|\Psi^B|} < \begin{cases} 1.5 \times 10^{-8} & (m^B/m^A = 2, 4, 5), \\ 7.7 \times 10^{-7} & (m^B/m^A = 10), \end{cases}$$

$$\frac{\max(|\Psi^A(\cdot, \pm Z_1^A, \cdot)|, |\Psi^A(\cdot, \cdot, Z_\rho^A)|)}{\max|\Psi^A|} < 6.0 \times 10^{-9},$$

$$\frac{\max(|\Psi^B(\cdot, \pm Z_1^B, \cdot)|, |\Psi^B(\cdot, \cdot, Z_\rho^B)|)}{\max|\Psi^B|} < 2.2 \times 10^{-8},$$

for problem II.

Finally, we provide the information about the accuracy of the Chebyshev polynomial approximation with respect to  $X_0^A$ . The  $b_I$  obtained by the formula (51) with the coefficient  $b_I^{(n)}$  in Table I is compared with that computed directly. The comparison was made at 15 sample values of  $X_0^A$  for  $m^B/m^A=2$ , at 8 values for  $m^B/m^A=4$ , at 12 values for  $m^B/m^A=5$ , and at 4 values for  $m^B/m^A=10$ . The relative errors to the directly computed data are, at most,  $3 \times 10^{-6}$ ,  $9 \times 10^{-8}$ ,  $4 \times 10^{-7}$ , and  $2 \times 10^{-7}$ , respectively. The corresponding comparison was made for  $b_{II}$  at 4 sample values of  $X_0^A$  for  $m^B/m^A=2$  and at 5 values for  $m^B/m^A=4, 5, 10$ . The relative errors are, at most,  $7 \times 10^{-9}$ ,  $3 \times 10^{-8}$ ,  $6 \times 10^{-8}$ , and  $2 \times 10^{-7}$ , respectively.

In the present work, we slightly improved the accuracy of numerical solutions in Refs. 12 and 25. The improvement was achieved chiefly by computing in a wider region of  $\zeta_\rho$  than that in Ref. 12 and by making the lattice system finer near  $\zeta_1=0$  than that in Ref. 25. As a result, some of the data of slip coefficients in those references are different from the present ones at the last figure.

## APPENDIX A: TRANSPORT COEFFICIENTS AND FUNCTIONS $A^\alpha$ AND $D^{(\beta)\alpha}$

The coefficients  $\hat{\lambda}^{\alpha'}$ ,  $\hat{\Delta}_{\alpha\beta}$ ,  $\hat{D}_{T\alpha}$ ,  $\hat{\Gamma}_D^{(\alpha)\beta}$ , and  $\hat{\lambda}'$  ( $\alpha, \beta = A, B$ ) are defined by the moments of  $A^\alpha$  or  $D^{(\beta)\alpha}$  as follows:

$$\hat{\lambda}^{\alpha'} = \frac{5}{2} I_4^\alpha \left( \left[ \hat{m}^\alpha \zeta^2 - \frac{5}{2} \right] A^\alpha \right),$$

$$\hat{\Delta}_{\alpha\beta} = \frac{5}{2} I_4^\alpha (D^{(\beta)\alpha}), \quad \hat{D}_{T\alpha} = \frac{5}{2} I_4^\alpha (A^\alpha),$$

$$\hat{\Gamma}_D^{(\beta)\alpha} = \frac{5}{2} I_4^\alpha \left( \left[ \hat{m}^\alpha \zeta^2 - \frac{5}{2} \right] D^{(\beta)\alpha} \right),$$

$$\hat{\lambda}' = X_0^A \hat{\lambda}^{A'} + X_0^B \hat{\lambda}^{B'},$$

where

$$I_n^\alpha(F) = \frac{8\pi}{15} \int_0^\infty \zeta^n F E^\alpha d\zeta. \quad (A2)$$

Since  $\hat{m}^A = \hat{d}^A = 1$  and  $X_0^B = 1 - X_0^A$ , they are functions of  $X_0^A$ ,  $\hat{m}^B$ , and  $\hat{d}^B$  [see the definitions of  $A^\alpha$  and  $D^{(\beta)\alpha}$  in Eqs. (9a) and (9b)]. There are some relations among  $\hat{\Delta}_{\alpha\beta}$ ,  $\hat{D}_{T\alpha}$ , and  $\hat{\Gamma}_D^{(\alpha)\beta}$ :

$$\hat{\Delta}_{\alpha\beta} = \hat{\Delta}_{\beta\alpha}, \quad \hat{D}_{T\alpha} = X_0^A \hat{\Gamma}_D^{(\alpha)A} + X_0^B \hat{\Gamma}_D^{(\alpha)B},$$

$$\hat{m}^A X_0^A \hat{\Delta}_{\alpha A} + \hat{m}^B X_0^B \hat{\Delta}_{\alpha B} = 0, \quad (A3)$$

$$\hat{m}^A X_0^A \hat{D}_{TA} + \hat{m}^B X_0^B \hat{D}_{TB} = 0.$$

The last two relations are the subsidiary conditions for  $A^\alpha$  and  $D^{(\beta)\alpha}$  [see Eqs. (9a) and (9b)]. The  $\hat{\Delta}_{\alpha\beta}$  and  $\hat{D}_{T\alpha}$  are directly related to the generalized diffusion coefficient<sup>42</sup>  $\Delta_{\alpha\beta}$  and the thermal diffusion coefficient<sup>42</sup>  $D_{T\alpha}$  as follows:

$$\Delta_{\alpha\beta} = (\sqrt{\pi}/2) \hat{\Delta}_{\alpha\beta} (2kT_0/m^A)^{1/2} l_0, \quad (A4)$$

$$D_{T\alpha} = (\sqrt{\pi}/2) \hat{D}_{T\alpha} (2kT_0/m^A)^{1/2} l_0.$$

The reader is referred to Appendix A in Refs. 56 and 5 for further details.

## APPENDIX B: EXPRESSION OF INTEGRAL KERNELS

Here we give the explicit expression of  $\mathcal{K}_J^{\beta\alpha}$  ( $J=1,2,3$ ) in Eq. (22):

$$\mathcal{K}_1^{\beta\alpha} = \begin{cases} \sqrt{\frac{2}{\pi}} \left( \frac{\hat{\mu}_-^{\beta\alpha}}{\hat{\mu}_+^{\beta\alpha}} \right)^2 \xi_\rho \mathcal{J}_1^{\beta\alpha}(\xi_1, \xi_\rho, \zeta_1, \zeta_\rho), & \text{if } \hat{m}^\alpha \neq \hat{m}^\beta, \\ \mathcal{K}_2^{\beta\alpha}, & \text{if } \hat{m}^\alpha = \hat{m}^\beta, \end{cases} \quad (B1)$$

$$\mathcal{K}_2^{\beta\alpha} = \left( \frac{\pi}{2} \hat{m}^\alpha \hat{m}^\beta \right)^{1/2} (\hat{\mu}^{\beta\alpha})^{-2} \xi_\rho e^{\hat{m}^\alpha |\xi|^2} \mathcal{J}_2^{\beta\alpha}(\xi_1, \xi_\rho, \zeta_1, \zeta_\rho), \quad (B2)$$

$$\mathcal{K}_3^{\beta\alpha} = \frac{\sqrt{2}\pi}{3k} \xi_\rho [(\xi_1 - \zeta_1)^2 + (\xi_\rho + \zeta_\rho)^2]^{1/2} \times [(k-2)E(k) + 2(1-k)F(k)], \quad (B3)$$

with

$$\mathcal{J}_1^{\beta\alpha} = \int_0^\pi d\varphi_\xi \cos \varphi_\xi |\xi - \zeta| I_1^{\beta\alpha}(\xi_1, \xi_\rho, \varphi_\xi, \zeta_1, \zeta_\rho), \quad (B4)$$

$$\mathcal{J}_2^{\beta\alpha} = \int_0^\pi d\varphi_\xi \frac{\cos \varphi_\xi}{|\xi - \zeta|} I_2^{\beta\alpha}(\xi_1, \xi_\rho, \varphi_\xi, \zeta_1, \zeta_\rho), \quad (\text{B5})$$

$$I_1^{\beta\alpha} = e^{-a^{\beta\alpha}} \int_0^1 dt \cosh(-a^{\beta\alpha}t) \times \int_0^{\pi/2} ds \cosh(b^{\beta\alpha} \sqrt{1-t^2} \sin s), \quad (\text{B6})$$

$$I_2^{\beta\alpha} = \exp\left(-\frac{\hat{m}^\beta}{4} \left(\frac{\hat{m}^\alpha}{\hat{m}^\beta} |\xi - \zeta| + \frac{|\zeta|^2 - |\xi|^2}{|\xi - \zeta|}\right)^2\right), \quad (\text{B7})$$

and

$$a^{\beta\alpha} = (\hat{\mu}_-^{\beta\alpha})^2 \left( \frac{|\xi|^2}{2\hat{m}^\alpha} + \frac{|\zeta|^2}{2\hat{m}^\beta} - \frac{\xi \cdot \zeta}{\hat{\mu}_-^{\beta\alpha}} \right), \quad (\text{B8})$$

$$b^{\beta\alpha} = -\hat{\mu}_-^{\beta\alpha} |\xi \times \zeta|, \quad (\text{B9})$$

$$\hat{\mu}_-^{\beta\alpha} = \frac{2\hat{m}^\beta \hat{m}^\alpha}{\hat{m}^\beta - \hat{m}^\alpha}, \quad \text{for } \hat{m}^\beta \neq \hat{m}^\alpha, \quad (\text{B10})$$

$$k = \frac{4\xi_\rho \zeta_\rho}{(\xi_1 - \zeta_1)^2 + (\xi_\rho + \zeta_\rho)^2}. \quad (\text{B11})$$

The functions  $F$  and  $E$  in Eq. (B3) are, respectively, the complete elliptic integrals of the first and the second kinds<sup>54</sup> defined by

$$F(k) = \int_0^{\pi/2} (1 - k \sin^2 \theta)^{-1/2} d\theta, \quad (\text{B12})$$

$$E(k) = \int_0^{\pi/2} (1 - k \sin^2 \theta)^{1/2} d\theta. \quad (\text{B13})$$

In the above expressions, the absolute values of vectors and the inner product of  $\xi$  and  $\zeta$  are expressed in terms of  $\zeta_1$ ,  $\zeta_\rho$ ,  $\xi_1$ ,  $\xi_\rho$ , and  $\varphi_\xi$  as follows:

$$\begin{aligned} |\xi - \zeta| &= (|\xi|^2 + |\zeta|^2 - 2\xi \cdot \zeta)^{1/2}, \\ |\xi \times \zeta| &= [|\xi|^2 |\zeta|^2 - (\xi \cdot \zeta)^2]^{1/2}, \\ |\xi|^2 &= \xi_1^2 + \xi_\rho^2, \quad |\zeta|^2 = \zeta_1^2 + \zeta_\rho^2, \\ \xi \cdot \zeta &= \xi_1 \zeta_1 + \xi_\rho \zeta_\rho \cos \varphi_\xi. \end{aligned} \quad (\text{B14})$$

### APPENDIX C: PROOF OF NO DIFFUSION SLIP FOR THE MIXTURE OF IDENTICAL MOLECULES

When the molecules of different species are mechanically identical, i.e.,  $m^B/m^A = d^B/d^A = 1$ ,  $\tilde{L}^{\beta\alpha}$  is reduced to the collision operator for a single-component gas, say  $\tilde{L}$ , and the relation

$$\sum_{\alpha=A,B} X_0^\alpha [D^{(A)\alpha}(\zeta) - D^{(B)\alpha}(\zeta)] = 0,$$

holds.<sup>56</sup> As a result, by adding Eqs. (12), (13b), and (14) for  $\alpha=A$  and those for  $\alpha=B$ , respectively, one obtains the following boundary-value problem for  $\Psi = \Psi^A + \Psi^B$ :

$$\zeta_1 \frac{\partial \Psi}{\partial x_1} = \tilde{L}(\Psi), \quad (\text{C1})$$

$$\Psi = -2\zeta_2 b_{II}, \quad \zeta_1 > 0, \quad x_1 = 0, \quad (\text{C2a})$$

$$\Psi \rightarrow 0, \quad \text{as } x_1 \rightarrow \infty, \quad (\text{C2b})$$

where  $\tilde{L}(f) = \tilde{L}^{\beta\alpha}(f, f)$  with  $\hat{m}^\beta = \hat{m}^\alpha = 1$ . This is the Knudsen-layer problem for a single-component gas, and thus there is the theorem for the existence and uniqueness of the solution (see Sec. III B). Since the set  $\Psi = 0$  and  $b_{II} = 0$  is seen to satisfy Eqs. (C1)–(C2b),  $\Psi = 0$  is the unique solution, and the diffusion-slip flow is not induced ( $b_{II} = 0$ ).

<sup>1</sup>Y. Sone, "Asymptotic theory of flow of rarefied gas over a smooth boundary I," in *Rarefied Gas Dynamics*, edited by L. Trilling and H. Y. Wachman (Academic, New York, 1969), Vol. I, p. 243.

<sup>2</sup>Y. Sone, "Asymptotic theory of flow of rarefied gas over a smooth boundary II," in *Rarefied Gas Dynamics*, edited by D. Dini (Editrice Tecnica Scientifica, Pisa, 1971), Vol. II, p. 737.

<sup>3</sup>Y. Sone, "Asymptotic theory of a steady flow of a rarefied gas past bodies for small Knudsen numbers," in *Advances in Kinetic Theory and Continuum Mechanics*, edited by R. Gatignol and Soubbaramayer (Springer-Verlag, Berlin, 1991), p. 19.

<sup>4</sup>Y. Sone, *Kinetic Theory and Fluid Dynamics*, Modeling and Simulation in Science, Engineering and Technology (Birkhäuser, Boston, 2002).

<sup>5</sup>S. Takata and K. Aoki, "The ghost effect in the continuum limit for a vapor-gas mixture around condensed phases: Asymptotic analysis of the Boltzmann equation," *Transp. Theory Stat. Phys.* **30**, 205 (2001); erratum, *ibid.* **31**, 289 (2002).

<sup>6</sup>Y. Sone, K. Aoki, S. Takata, H. Sugimoto, and A. V. Bobylev, "Inappropriateness of the heat-conduction equation for description of a temperature field of a stationary gas in the continuum limit: Examination by asymptotic analysis and numerical computation of the Boltzmann equation," *Phys. Fluids* **8**, 628 (1996); erratum, *ibid.* **8**, 841 (1996).

<sup>7</sup>Y. Sone, "Continuum gas dynamics in the light of kinetic theory and new features of rarefied gas flows," in *Rarefied Gas Dynamics*, edited by C. Shen (Peking University Press, Beijing, 1997), p. 3.

<sup>8</sup>Y. Sone, "Flows induced by temperature fields in a rarefied gas and their ghost effect on the behavior of a gas in the continuum limit," *Annu. Rev. Fluid Mech.* **32**, 779 (2000).

<sup>9</sup>E. H. Kennard, *Kinetic Theory of Gases* (McGraw-Hill, New York, 1938).

<sup>10</sup>H. A. Kramers and J. Kistemaker, "On the slip of a diffusing gas mixture along a wall," *Physica (Amsterdam)* **10**, 699 (1943).

<sup>11</sup>Y. Sone, T. Ohwada, and K. Aoki, "Temperature jump and Knudsen layer in a rarefied gas over a plane wall: Numerical analysis of the linearized Boltzmann equation for hard-sphere molecules," *Phys. Fluids A* **1**, 363 (1989).

<sup>12</sup>T. Ohwada, Y. Sone, and K. Aoki, "Numerical analysis of the shear and thermal creep flows of a rarefied gas over a plane wall on the basis of the linearized Boltzmann equation for hard-sphere molecules," *Phys. Fluids A* **1**, 1588 (1989).

<sup>13</sup>T. Ohwada, K. Aoki, and Y. Sone, "Heat transfer and temperature distribution in a rarefied gas between two parallel plates with different temperatures: Numerical analysis of the Boltzmann equation for a hard sphere molecule," in *Rarefied Gas Dynamics: Theoretical and Computational Techniques*, edited by E. P. Muntz, D. P. Weaver, and D. H. Campbell (AIAA, Washington, DC, 1989), p. 70.

<sup>14</sup>Y. Sone, T. Ohwada, and K. Aoki, "Evaporation and condensation on a plane condensed phase: Numerical analysis of the linearized Boltzmann equation for hard-sphere molecules," *Phys. Fluids A* **1**, 1398 (1989).

<sup>15</sup>T. Ohwada, Y. Sone, and K. Aoki, "Numerical analysis of the Poiseuille and thermal transpiration flows between two parallel plates on the basis of the Boltzmann equation for hard-sphere molecules," *Phys. Fluids A* **1**, 2042 (1989).

<sup>16</sup>Y. Sone, S. Takata, and T. Ohwada, "Numerical analysis of the plane Couette flow of a rarefied gas on the basis of the linearized Boltzmann equation for hard-sphere molecules," *Eur. J. Mech. B/Fluids* **9**, 273 (1990).

<sup>17</sup>Y. Sone, T. Ohwada, and K. Aoki, "Evaporation and condensation of a rarefied gas between its two parallel plane condensed phases with different temperatures and negative temperature-gradient phenomenon: Numerical analysis of the Boltzmann equation for hard-sphere molecules," in *Mathematical Aspects of Fluid and Plasma Dynamics*, Lecture Notes in Math-

- ematics Vol. 1460, edited by G. Toscani, V. Boffi, and S. Rionero (Springer-Verlag, Berlin, 1991), p. 186.
- <sup>18</sup>T. Ohwada and Y. Sone, "Analysis of thermal stress slip flow and negative thermophoresis using the Boltzmann equation for hard-sphere molecules," *Eur. J. Mech. B/Fluids* **11**, 389 (1992).
- <sup>19</sup>S. Takata, Y. Sone, and K. Aoki, "Numerical analysis of a uniform flow of a rarefied gas past a sphere on the basis of the Boltzmann equation for hard-sphere molecules," *Phys. Fluids A* **5**, 716 (1993).
- <sup>20</sup>S. Takata, K. Aoki, and Y. Sone, "Thermophoresis of a sphere with a uniform temperature: Numerical analysis of the Boltzmann equation for hard-sphere molecules," in *Rarefied Gas Dynamics: Theory and Simulations*, edited by B. D. Shizgal and D. P. Weaver, Vol. 159 of Progress in Astronautics and Aeronautics (AIAA, Washington, DC, 1994), p. 626.
- <sup>21</sup>Y. Sone, S. Takata, and M. Wakabayashi, "Numerical analysis of a rarefied gas flow past a volatile particle using the Boltzmann equation for hard-sphere molecules," *Phys. Fluids* **6**, 1914 (1994).
- <sup>22</sup>S. Takata and Y. Sone, "Flow induced around a sphere with a non-uniform surface temperature in a rarefied gas, with application to the drag and thermal force problems of a spherical particle with an arbitrary thermal conductivity," *Eur. J. Mech. B/Fluids* **14**, 487 (1995).
- <sup>23</sup>M. Wakabayashi, T. Ohwada, and F. Golse, "Numerical analysis of the shear and thermal creep flows of a rarefied gas over the plane wall of a Maxwell-type boundary on the basis of the linearized Boltzmann equation for hard-sphere molecules," *Eur. J. Mech. B/Fluids* **15**, 175 (1996).
- <sup>24</sup>S. Takata, Y. Sone, D. Lhuillier, and M. Wakabayashi, "Evaporation from or condensation onto a sphere: Numerical analysis of the Boltzmann equation for hard-sphere molecules," *Comput. Math. Appl.* **35**, 193 (1998).
- <sup>25</sup>S. Takata, "Diffusion slip for a binary mixture of hard-sphere molecular gases: Numerical analysis based on the linearized Boltzmann equation," in *Rarefied Gas Dynamics*, edited by T. J. Bartel and M. A. Gallis (American Institute of Physics, Melville, NY, 2001), p. 22.
- <sup>26</sup>Y. Sone, "Thermal creep in rarefied gas," *J. Phys. Soc. Jpn.* **21**, 1836 (1966).
- <sup>27</sup>V. M. Zhdanov, "Theory of slip at the boundary of a gaseous mixture," *Sov. Phys. Tech. Phys.* **12**, 134 (1967).
- <sup>28</sup>L. Waldmann and K. H. Schmitt, "Über das bei der Gasdiffusion auftretende Druckgefälle," *Z. Naturforsch.* **16a**, 1343 (1961).
- <sup>29</sup>S. K. Loyalka, "Velocity slip coefficient and the diffusion slip velocity for a multicomponent gas mixture," *Phys. Fluids* **14**, 2599 (1971).
- <sup>30</sup>Y. Onishi, "On the behavior of a slightly rarefied gas mixture over plane boundaries," *Z. Angew. Math. Phys.* **37**, 573 (1986).
- <sup>31</sup>S. K. Loyalka, "Temperature jump and thermal creep slip: Rigid sphere gas," *Phys. Fluids A* **1**, 403 (1989).
- <sup>32</sup>I. V. Volkov and V. S. Galkin, "Analysis of slip and temperature jump coefficients in a binary gas mixture," *Fluid Dyn.* **25**, 937 (1990).
- <sup>33</sup>Yu. I. Yalamov, A. A. Yushkanov, and S. A. Savkov, "Boundary conditions for the slippage of a binary mixture of gases and their application in the dynamics of aerosols. 1. Flow of a mixture of gases along a solid plane wall," *J. Eng. Phys. Thermophys.* **66**, 367 (1994).
- <sup>34</sup>I. N. Ivchenko, S. K. Loyalka, and R. V. Tompson, "Slip coefficients for binary gas mixtures," *J. Vac. Sci. Technol. A* **15**, 2375 (1997).
- <sup>35</sup>C. M. Huang, R. V. Tompson, T. K. Ghosh, I. N. Ivchenko, and S. K. Loyalka, "Measurements of thermal creep in binary gas mixtures," *Phys. Fluids* **11**, 1662 (1999).
- <sup>36</sup>C. E. Siewert, "Two half-space problems based on a synthetic-kernel model of the linearized Boltzmann equation," *J. Quant. Spectrosc. Radiat. Transf.* **75**, 21 (2002).
- <sup>37</sup>C. E. Siewert and F. Sharipov, "Model equations in rarefied gas dynamics: Viscous-slip and thermal-slip coefficients," *Phys. Fluids* **14**, 4123 (2002).
- <sup>38</sup>I. N. Ivchenko, S. K. Loyalka, and R. V. Tompson, "Boundary slip phenomena in a binary gas mixture," *Z. Angew. Math. Phys.* **53**, 58 (2002).
- <sup>39</sup>F. Sharipov and D. Kalempa, "Slip coefficients for gaseous mixture," in *Rarefied Gas Dynamics*, edited by A. D. Ketsdever and E. P. Muntz (American Institute of Physics, Melville, NY, 2003), p. 164.
- <sup>40</sup>C. E. Siewert, "Viscous-slip, thermal-slip, and temperature-jump coefficients as defined by the linearized Boltzmann equation and the Cercignani-Lampis boundary condition," *Phys. Fluids* **15**, 1696 (2003).
- <sup>41</sup>M. N. Kogan, *Rarefied Gas Dynamics* (Plenum, New York, 1969).
- <sup>42</sup>S. Chapman and T. G. Cowling, *The Mathematical Theory of Non-Uniform Gases*, 3rd ed. (Cambridge University Press, Cambridge, 1995).
- <sup>43</sup>J. O. Hirschfelder, C. F. Curtiss, and R. B. Bird, *Molecular Theory of Gases and Liquids* (Wiley, New York, 1954).
- <sup>44</sup>S. Takata, S. Yasuda, K. Aoki, and T. Shibata, "Various transport coefficients occurring in binary gas mixtures and their database," in Ref. 39, p. 106.
- <sup>45</sup>K. Aoki, C. Bardos, and S. Takata, "Knudsen layer for gas mixtures," *J. Stat. Phys.* **112**, 629 (2003).
- <sup>46</sup>H. Grad, "Singular and nonuniform limits of solutions of the Boltzmann equation," in *Transport Theory*, edited by R. Bellman, G. Birkhoff, and I. Abu-Shumays (AMS, Providence, RI, 1969), p. 269.
- <sup>47</sup>N. B. Maslova, "Kramers problem in the kinetic theory of gases," *USSR Comput. Math. Math. Phys.* **22**, 208 (1982).
- <sup>48</sup>C. Bardos, R. E. Caflisch, and B. Nicolaenko, "The Milne and Kramers problems for the Boltzmann equation of a hard sphere gas," *Commun. Pure Appl. Math.* **39**, 323 (1986).
- <sup>49</sup>C. Cercignani, "Half-space problems in the kinetic theory of gases," in *Trends in Applications of Pure Mathematics to Mechanics*, edited by E. Kröner and K. Kirchgässner (Springer-Verlag, Berlin, 1986), p. 35.
- <sup>50</sup>F. Coron, F. Golse, and C. Sulem, "A classification of well-posed kinetic layer problems," *Commun. Pure Appl. Math.* **41**, 409 (1988).
- <sup>51</sup>F. Golse and F. Poupaud, "Stationary solutions of the linearized Boltzmann equation in a half-space," *Math. Methods Appl. Sci.* **11**, 483 (1989).
- <sup>52</sup>H. Grad, "Asymptotic theory of the Boltzmann equation, II," in *Rarefied Gas Dynamics*, edited by J. A. Laurmann (Academic, New York, 1963), Vol. I, p. 26.
- <sup>53</sup>Y. Sone and S. Takata, "Discontinuity of the velocity distribution function in a rarefied gas around a convex body and the S layer at the bottom of the Knudsen layer," *Transp. Theory Stat. Phys.* **21**, 501 (1992).
- <sup>54</sup>M. Abramowitz and I. A. Stegun, *Handbook of Mathematical Functions* (Dover, New York, 1968).
- <sup>55</sup>C. Gasquet and P. Witomski, *Fourier Analysis and Applications* (Springer-Verlag, New York, 1999).
- <sup>56</sup>S. Takata and K. Aoki, "Two-surface problems of a multicomponent mixture of vapors and noncondensable gases in the continuum limit in the light of kinetic theory," *Phys. Fluids* **11**, 2743 (1999).
- <sup>57</sup>F. J. McCormack, "Construction of linearized kinetic models for gaseous mixtures and molecular gases," *Phys. Fluids* **16**, 2095 (1973).
- <sup>58</sup>S. K. Loyalka and K. A. Hickey, "The Kramers problem: Velocity slip and defect for a hard sphere gas with arbitrary accommodation," *Z. Angew. Math. Phys.* **41**, 245 (1990).
- <sup>59</sup>C. Cercignani and M. Lampis, "Kinetic model for gas-surface interaction," *Transp. Theory Stat. Phys.* **1**, 101 (1971).